

MINISTRY OF SUPPLY

AERONAUTICAL RESEARCH COUNCIL

CURRENT PAPERS

The Determination of Skin Temperatures Attained in High Speed Flight

By

F. V. Davies and R. J. Monaghan

LONDON: HER MAJESTY'S STATIONERY OFFICE

1953

Price 12s. 6d. net

Report No. Aero 2454

February, 1952

ROYAL AIRCRAFT ESTABLISHMENT

The estimation of skin temperatures
attained in high speed flight

by

F.V. Davies
and
R.J. Monaghan

SUMMARY

This report discusses the factors affecting skin temperatures attained by high speed missiles and presents some methods of solution. These have been reduced to graphical or tabular form and are set out in order of complexity.

Graphical or algebraic solutions may be quickly obtained if steady conditions are assumed, and for some flight cases these are reasonable approximations to corresponding transient solutions. If the temperature time variation is required then longer numerical integration processes have to be performed.

Account may be taken of external radiation and heat loss to the interior if their effects are considered significant.

Although the emphasis of this report is on the calculation of average temperatures attained by thin skins, a method of calculating the temperature-space-time variation through 3 dimensional bodies has been included assuming steady conditions at the surface.

Numerical examples are included for each section of the report.

LIST OF CONTENTS

	<u>Page</u>
1 Introduction	7
2 Stagnation and Equilibrium Temperatures	8
2.1 Stagnation temperature	8
2.2 Kinetic temperature	8
2.3 Equilibrium temperature	9
3 Transient temperatures for a thin skin with no heat loss to interior of body	12
3.1 Completely turbulent or completely laminar layers	13
3.11 Wings and cylindrical afterbodies	13
3.12 Nose cones or ogives	14
3.13 Examples	14
3.2 Cases with transition or changes in body geometry	15
4 Transient temperatures for thin skins with heat loss to the interior or for a sandwich type construction	15
5 Temperature distribution in thick skins	17
References	18

LIST OF APPENDICES

	<u>Appendix</u>
Stagnation and kinetic temperature rises	I
Derivation of aerodynamic heat transfer coefficients	II
A method of numerical integration	III
Calculation of transient temperatures for a wing or cylindrical body, using the integration method of Appendix III	IV
Calculation of transient skin temperatures for a cone or ogive	V
Calculation of transient skin temperatures on a missile with a discontinuity in body geometry or a boundary layer transition	VI
The temperature distribution through a semi infinite slab at constant initial temperature T with its surface temperature suddenly raised to and maintained at a constant value T_{wo}	VII
Sources of data used	VIII
The effect of the boundary layer character on heat transfer	IX

LIST OF TABLES

	<u>Table</u>
The standard atmosphere below 100,000 ft	I
Material properties	II
Emmissivities	III
Temperature time space distribution through a semi infinite body	IV
Numerical solution of the transient skin temperature equation for a turbulent boundary layer on a flat plate or thin aerofoil	V
Numerical solution of the transient skin temperature equation for a turbulent boundary layer on a conical or ogival body	VI
Values of $\left(\frac{T_1}{T_w}\right)^{2.2/5}$ and $\left(\frac{T_1}{T_w}\right)^{1/10}$	VII
Numerical solution of the transient skin temperatures of a thin aerofoil with a turbulent boundary layer	VIII

LIST OF ILLUSTRATIONS

	<u>Figure</u>
Standard atmosphere (temperature and relative density)	1
Variation of viscosity of air with temperature	2
Variation of specific heat of air at constant pressure with temperature	3
Stagnation and kinetic temperature rises (variable c_p)	4a,4b,4c,4d
Approximate determination of equilibrium temperature	5
Nomogram giving variation of Reynolds number with speed and height	6
Heat transfer coefficients for the laminar boundary layer	7a
Heat transfer coefficients for the turbulent boundary layer	7b
Static temperature at surface of cone	8a
Density at surface of cone	8b
Velocity over cones	8c
Theoretical relation between the boundary layer characteristics of a tangent ogive and a flat plate	9
Average temperature of a cylinder and plate	10
Temperature space time distribution through a semi infinite body	11

LIST OF ILLUSTRATIONS (Contd.)

	<u>Figure</u>
Variation of $Re_{xt} - Re_{x0}$ with Re_{xt}	12
Comparison of kinetic and equilibrium temperatures on a wing	13
Transient skin temperatures for a flat plate wing in accelerated flight at sea level (case A)	14
Transient skin temperatures for a flat plate wing in accelerated flight at varying altitude (case B)	15
Transient skin temperatures for a conical forebody (turbulent boundary layer) in accelerated flight at sea level (case C)	16
Transient skin temperatures for a conical forebody (laminar boundary layer) in accelerated flight at sea level (case D)	17
Reynolds number variations associated with examples in Figs.14-17	18

NOTATION

<u>Symbol</u>	<u>Description</u>	<u>Units</u>
c_p	specific heat of air	CHU/lb °C
c_s	specific heat of solid	CHU/lb °C
ρ_{SLg}	air density at sea level	lb/ft ³
σ	relative density ρ/ρ_{SL}	-
ρ_{sg}	density of solid	lb/ft ³
u	velocity	ft/sec
a	speed of sound in air	ft/sec
J	mechanical equivalent of heat	lb ft/CHU
T	temperature	°C abs.
T_H	stagnation temperature	°C abs.
T_{wo}	kinetic temperature	°C abs.
T_w	average skin temperature	°C abs.
\bar{T}	mean temperature of inner skin or interior	°C abs.
t	time	
Q	heat flow rate	CHU/sec
S	area	ft ²
Q_s	solar constant	CHU/ft ² sec
k_H	overall heat transfer coefficient	-
C_F	overall skin friction coefficient	-
τ	skin thickness	ft
G	$c_s \rho_s g \tau$	CHU/ft ² °C
B	Boltzmanns constant	CHU/ft ² sec (°K) ⁴
ϵ	emissivity factor	-
α_s	absorption factor for solar radiation	-
Re	Reynolds No./ft	1/ft
Re_x	Reynolds No.	-
Re_{xt}	Reynolds No. of transition	-
μ_g	viscosity	lb/ft sec

NOTATION (Cont'd.)

<u>Symbol</u>	<u>Description</u>	<u>Units</u>
ν	kinematic viscosity μ/ρ	ft ² /sec
ℓ	length	ft
h	increment in time	sec
k	thermal conductivity	CHU/°C ft sec
Pr	Prandtl No. $\mu c_p/k$	-
α	$k/\rho_s g c_s$	ft ² /sec
δ	boundary layer thickness	ft
r	cross section radius	ft
R	$\int dx/k$	ft ² sec °C/CHU
λ	coefficient of cubic thermal expansion	1/°C

Subscripts

SL	sea level conditions
o	ambient condition at height
1	conditions just outside the boundary layer
P	any point in a semi infinite body
i	initial value
w	conditions taken at skin temperature T_w
we	equilibrium skin conditions
s	refers to solids
n	conditions taken at time $(t)_n$

1 Introduction

When relative motion exists between air and a body, a layer of air adjacent to the body is retarded by viscous forces*, causing a rise in air temperature as the surface of the body is approached. Heat may then be transferred to the body (a phenomenon known as aerodynamic heating) and the temperature of the body will rise to an equilibrium value if the external flow conditions are steady.

A rough estimate of the ultimate rise in body temperature is given in degrees centigrade by $(u_1/100)^2$ where u_1 is the speed in miles per hour. Thus at 100 m.p.h. the temperature rise is only about 1°C, but at 1000 m.p.h. it has increased to the order of 100°C, which illustrates why aerodynamic heating assumes importance in high speed flight.

The equilibrium case is relatively simple to calculate, but in many cases the external conditions are varying and the flight duration is short, so that it is necessary to determine the variation of surface temperature throughout the flight. The wide range of flight plans, boundary layer conditions, body geometries, constructions and materials makes it impossible to present transient solutions in a general form. This note sets out the general problem and gives a numerical method of solution for the average skin temperature. Graphs and Tables are included to reduce as much as possible the labour involved in the computations.

The sequence of the calculations may be described briefly as follows.

- (a) calculation of equilibrium temperatures for a given set of steady external conditions (e.g. the maximum speed at which the missile may operate),
- (b) calculation of transient temperatures of thin skins assuming a completely turbulent or completely laminar boundary layer and no changes in the body geometry,
- (c) calculation of transient temperatures of thin skins allowing for transition from laminar to turbulent flow, and for changes in the body geometry (e.g. from nose cone or ogive to cylindrical afterbody),
- (d) calculations allowing for heat loss to the interior of the body or for sandwich type construction.

The calculations increase in complexity with the stages in this sequence, but in general the temperatures obtained from any stage will be less than those of the preceding stage so that in any particular problem the calculations need only be carried as far as may be required.

The application of this note covers speeds from 0 to 4000 ft/sec and altitudes from 0 to 100,000 ft. For speeds and heights in excess of these limits reference should be made to the papers of Nonweiler⁶ and Stalder and Jukoff¹⁴. It is assumed in general that the missiles are thin skinned since the problem of temperature-space-time variation through a thick skin is extremely complicated if the external conditions are unsteady. However, standard analytical solutions are available for the latter case under steady external conditions and a solution with practical applications is presented in section 6 and Appendix VII.

*Except at the stagnation point where there is pure compression, also giving a rise in temperature.

2 Stagnation, kinetic and equilibrium temperatures

This section covers the first stage in the calculations and for a given speed and altitude will give upper limits to the body temperatures. The highest estimate is given by the stagnation temperature, but lower and more accurate estimates are given successively by the kinetic and then the equilibrium temperatures. Needless to say, if any of these estimates are acceptable then no further work is necessary. The derivation of the results is given in Appendix I.

2.1 Stagnation temperature

The stagnation temperature of a moving fluid is that attained when the flow is adiabatically brought to rest*. This occurs theoretically at the stagnation point of a body, but in practice a somewhat lower temperature is attained in this region.

Bearing this in mind, Fig.4 gives the rise in stagnation temperature of air above ambient temperature plotted against speed. (All the curves in Fig.4 allow for the variation in the specific heat of air with temperature). The stagnation temperature itself is then obtained by adding to this rise the ambient temperature for the height in question (Table I).

For example, for a speed of 2,000 ft/sec and an altitude of 33,000 ft, Fig.4b gives a temperature rise of 183°C and Table I gives the ambient temperature to be -50.34°C so that the stagnation temperature would be approximately 133°C.

Also plotted on Fig.4a are spot values from the rough relation mentioned in the introduction

$$\text{Temperature rise} = \left(\frac{u_1}{100} \right)^2 \text{ } ^\circ\text{C}$$

where u_1 is in miles per hour.

$$(1 \text{ ft/sec} = 0.6818 \text{ m.p.h.})$$

and these are seen to be in good agreement with the stagnation temperature rise for speeds at least up to 2,500 ft/sec. (At 2,500 ft/sec the rough relation is 5°C high).

2.2 Kinetic temperature

This is the temperature rise experienced under zero heat transfer conditions as the surface of the body is approached through the boundary layer. The fluid in contact with the surface of the body is at rest relative to the body, but in general the full stagnation temperature rise is not obtained because of the conflicting actions of viscosity and thermal conductivity in the adjacent boundary layer. The percentage of the rise obtained (relative to the static temperature outside the boundary layer) has been shown experimentally and theoretically to be dependent on

* In practice the body will be moving through air initially at rest, but it simplifies discussion if we consider the motion relative to the body.

the Prandtl number ($c_p \mu / k$) of the fluid. If the Prandtl number is less than unity (it is approximately 0.72 for air) the kinetic temperature rise is less than the stagnation temperature rise, the ratios being about 0.90 for turbulent and 0.85 for laminar boundary layers. These rises are plotted in Fig.4.

Thus for the example of section 2.1 the final temperature to be expected with a turbulent layer would be 115°C, while for a laminar layer it would be 106°C.

2.3 Equilibrium temperature

Under steady conditions and without internal cooling, the skin temperature would eventually reach the kinetic temperature of the adjacent boundary layer if there was no heat transfer to and from the skin by radiation. In practice an equilibrium condition will be reached when the convective heat transfer balances the radiative heat transfer. This is so when the mean skin temperature (T_w) satisfies the equation.

$$c_{pw} \rho_1 g u_1 k_H (T_{wo} - T_w) - \epsilon B T_w^4 + \alpha_s Q_s \cos \phi = 0 \quad (1)$$

(This equation is the particular case $\frac{dT_w}{dt} = 0$ of the general heat transfer equation of section 3.1 below, with the solar radiation term added).

Equation (1) can be solved graphically or numerically to give an equilibrium value of $T_w = T_{wc}$. Of the factors in it,

(a) $\frac{c_{pw} \rho_1 g u_1 k_H (T_{wo} - T_w)}$ represents the convective heat transfer to the skin from the boundary layer.

T_{wo} is the kinetic temperature (°K) determined in section 2.2

c_{pw} is the specific heat of air at constant pressure, evaluated at skin temperature T_w . (Fig.3)

$\rho_1 g$ is the weight density (lb/ft³) of the ambient air, which can be obtained from the relative density column of Table I in conjunction with the sea level value of 0.07652 lb/ft³

u_1 is the flight speed (ft/sec). (Strictly speaking, u_1 is the air velocity outside the boundary layer, but for convenience it may be taken at this stage to be the flight speed)

and k_H is the aerodynamic heat transfer coefficient, which can be determined from Fig.7 in conjunction with Fig.6 and Table VII (see also Appendix II).

(b) $\frac{\epsilon B T_w^4}$ represents the heat loss from the skin by radiation.

B is the Stefan-Boltzmann constant = $2.78 \times 10^{-12} \frac{\text{C.H.U.}}{\text{ft}^2 \cdot \text{sec} (\text{°K})^4}$

and ϵ is the emissivity factor. (Some values are given in Table III).

(c) $\frac{\alpha_s Q_s \cos \phi}{}$ represents the heat input to the skin by direct solar radiation. (Does not occur in a night flight).

Q_s is the solar constant (at outer limit of atmosphere)

$$= 6.82 \times 10^{-2} \frac{\text{C.H.U.}}{\text{ft}^2 \cdot \text{sec}}$$

(This is reduced by 6-8 per cent by the time the radiation reaches ground level)

α_s is the absorption factor for solar radiation, which differs from the emissivity ϵ . Thus for most polished metals α_s is about 0.4 whereas ϵ is about 0.05. Some values are given in Table III

and ϕ is the angle between the normal to the surface and the incident rays.

Note that direct solar radiation only affects those parts of the surface which can "see" the sun. A proportion of the incoming radiation is reflected by the earth and any clouds which are present and this will affect the undersurface of the wing or body. The reflection factor " A_s " is given approximately by Angström's formula

$$A_s = 0.70C + 0.17(1 - C)$$

where "C" is the cloud amount. (e.g. for $C = 0.5$, $A_s = 0.44$). This will apply over most land areas but if the ground is covered by snow and the sky is clear, then

$$A_s = 0.7 - 0.8$$

From this it follows that for the "undersurface" of the wing or body, the heat input by reflected solar radiation is given by

$$A_s \alpha_s Q_s \cos \phi.$$

In all the above discussion of solar radiation it is assumed that the aircraft or missile is flying above all cloud layers. If the flight is below a cloud level then it is probably best to neglect the solar radiation, since it will have undergone much scattering and diffuse reflection in passing through the cloud, and a quantitative estimate of its intensity would be very difficult.

2.31 Approximate estimate of equilibrium temperature

If we assume that T_{we} is not much different to T_{wo} , then as a first approximation the skin temperature dependent factors (c_{pw} and k_H) may be evaluated at the kinetic temperature T_{wo} , and equation (1) can be written

$$T_{wo} - T_{we} = A T_{we}^4 \quad (1a)$$

where

$$A = \frac{\epsilon B \left\{ 1 - \frac{\alpha_s Q_s \cos \phi}{\epsilon B T_{wo}^4} \right\}}{c_{pw} \rho_1 g u_1 k_H}$$

is constant.

The solution of equation (1a) to give the ratio $\frac{T_{we}}{T_{wo}}$ as a function of $A T_{wo}^3$ is given in Fig. 5. If necessary the values of T_{we} thus obtained may be improved by re-calculation of the value taken for A , preferably at some level intermediate between T_{wo} and T_{we} .

For the example of section 2.1 (i.e. a speed of 2,000 ft/sec at an altitude of 33,000 ft) applied to a wing of 4 ft chord we can thus obtain the following results for equilibrium temperature, if we assume that $\phi = 0$. (The Reynolds number is 2.3×10^7 , so the boundary layer is assumed to be turbulent, and in day time flight the results refer to the upper-surface. Heat transfer coefficient k_H was taken as for a flat plate, Fig. 7b).

Surface condition	T_{wo} °K	T_{we} °K	
		Day time	Night time ($\alpha_s = 0$)
Polished metal $\epsilon = 0.05$ $\alpha_s = 0.4$	388	400	388
Carbonised steel $\epsilon = 0.5$ $\alpha_s = 0.3$	388	388	386
Black body $\epsilon = 1.0$ $\alpha_s = 1.0$	388	388	384.5

Except for the polished metal skin in day time operation, the effects of radiation are small in this case. However at greater heights and speeds the effects become more pronounced as is shown by the results in Fig. 13, which were computed for a wing of 4 ft chord and emissivity factor 0.5 in night time operation ($\alpha_s = 0$).

Flat plate values were taken for k_H and transition was assumed to occur between 5 and 10 million Reynolds number, which corresponds to the shaded areas in Fig. 13a*. (Thus for $Re > 10$ million it is assumed that the influence of the laminar layer over the forward portion of the wing can be neglected when calculating the reductions in mean temperature. The shaded areas then represent the region of probable values for Reynolds numbers between 5 and 10 million).

The results show the benefits to be obtained at high speeds if the boundary layer can be kept laminar up to high Reynolds numbers and also that for speeds less than 3,000 ft/sec and altitudes less than 50,000 ft it may be permissible to neglect the radiation loss in subsequent calculations of transient temperatures.

*For clarity in plotting, transition was taken to occur at 7 million in Fig. 13b.

Note too that these results are for average temperature over the wing chord. The local temperatures will probably be higher than the average near the leading edge and lower than average near the trailing edge.

The effect of solar radiation in day time operation is indicated by the table above. In all cases its effect will be to increase the equilibrium temperature.

3 Transient temperatures of a thin skin with no heat loss to the interior of the body

In this case the heat balance at the surface of the body is made up as follows, (neglecting solar radiation):

1. Heat flowing into the skin from the air per square foot per second (aerodynamic heating)

$$\frac{Q_1}{S} = c_{pw} \rho_1 g u_1 k_H (T_{wo} - T_w) \quad (2)$$

(symbols are as in section 2.3)

2. Heat radiated per square foot per second from the skin to the surrounding air

$$\frac{Q_2}{S} = \epsilon B T_w^4 \quad (3)$$

(symbols as in section 2.3)

3. Heat absorbed by the skin per square foot per second

$$\begin{aligned} \frac{Q_3}{S} &= c_s \rho_s g \tau \frac{dT_w}{dt} \\ &= G \frac{dT_w}{dt} \end{aligned} \quad (4)$$

where c_s is specific heat of skin material C.H.U./lb °C

$\rho_s g$ is weight density of skin material lb/ft³

τ is skin thickness ft

t is time secs.

Thus G has the dimensions C.H.U./ft² °C, and typical values of it for a skin thickness of one foot are given in Table II.

The heat balance is then given by

$$Q_1 = Q_2 + Q_3$$

or
$$G \frac{dT_w}{dt} = c_{pw} \rho_1 g u_1 k_H (T_{wo} - T_w) - \epsilon B T_w^4 \quad (5)$$

which (even neglecting radiation) is in general a non-linear equation of which a general analytical solution cannot be found, so that a step by step integration has to be made.

A reasonably simple method for this integration is demonstrated in Appendices III, IV and V. In it c_{pw}/G and ϵ are taken to be constants for each part of the missile and the gravitational acceleration (g) is also taken to be constant with the altitude limits 0-100,000 ft. (In fact, g varies by 1 per cent in this range).

The aerodynamic heating term in equation (5) has purposely been left in its present form so that the general layout of the calculations need not be altered if more accurate heat transfer data become available at a future date. The sources of the present data are listed in Appendix VIII.

3.1 Completely turbulent or completely laminar boundary layers

Either case can be calculated by using the appropriate heat transfer coefficients (k_H) from Figs. 7a and 7b, in conjunction with the appropriate kinetic temperatures (T_{wo}) from Fig. 4 and Table I. A discussion of the factors influencing transition is given in Appendix IX, which indicates the present lack of quantitative data. Bearing this in mind, a rough guess would be to take the layer as laminar if the overall Reynolds number is less than 8 million. Since, however, the Reynolds number will in general be changing during the flight it may be thought preferable in doubtful cases to use turbulent values throughout. (This will give higher skin temperatures than may be obtained in practice with combined laminar and turbulent boundary layers). Calculations including transition are considered in section 3.2 below.

Following the equilibrium temperature results of section 2.3 it is probably justifiable to neglect the radiation term (equation (3)) in equation (5) for speeds less than 3,000 ft/sec approximately and altitudes less than 50,000 ft approximately, but an independent check should be made in doubtful cases.

3.11 Wings and cylindrical afterbodies (Appendix IV for calculation method)

For thin wings the effect of pressure gradients at the leading edge, along the aerofoil profile and at the wing root and tip, on the behaviour of the boundary layer is ignored in this Report and flat plate data used.

For relatively thick wings reference can be made to Squires paper¹³ if it is desired to account for the chordwise variation of heat transfer.

Flat plate data can also be used for cylindrical afterbodies whose cross-section radii are large compared with the boundary layer thickness. A rough guide to this is given by the formula

$$\frac{\delta}{r} = 0.38 \text{Re}^{-1/5} \frac{\ell}{r} < 0.1 \quad (6)$$

where δ is boundary layer thickness
 r is body cross section radius
 ℓ is body length.

3.12 Nose cones or ogives (Appendix V for calculation method)

The calculation for the cone or ogive is complicated by the change in physical characteristics of the flow through the shock wave at the tip. Before commencing the numerical integration it is necessary therefore to obtain the values of density, temperature and velocity immediately outside the boundary layer (Appendix V). The remainder of the calculation is very similar to that for the flat plate or aerofoil. It should be noted that the heat transfer coefficients for cones and ogives differ from the flat plate coefficient. The ogive-flat-plate heat transfer factor varies with tip angle (see Fig.9); the cone factor is constant so that $k_{H\text{cone}}$ is plotted with the flat plate coefficient (Fig.7).

3.13 Discussion of results of worked examples

Some examples of transient temperature curves have been calculated by the methods of Appendices III, IV and V and the results are shown in Figs.14-17, together with the relevant data and flight histories. Four cases are considered, in all of which a constant angle trajectory is assumed with constant acceleration for the first three seconds, followed by typical variations of velocity with time. The cases are,

- A. wing skin temperatures for flight at sea level, (Fig.14),
 - B. wing skin temperatures for a 45° trajectory from a sea level launch (Fig.15),
 - C. nose cone skin temperatures for flight at sea level assuming a turbulent boundary layer (Fig.16),
- and D as for case C, but with a laminar boundary layer (Fig.17).

The variations in overall Reynolds number for the four cases are given in Fig.18, which shows that only in case B towards the end of the flight is there likely to be any appreciable length of laminar boundary layer. Therefore turbulent boundary layer data were used throughout the calculations and case D was added purely for comparison purposes.

Preliminary estimates of kinetic and equilibrium temperatures showed that at maximum velocity (and height in case B) the reductions in temperature to be expected from radiation losses would amount to about 1°C in cases A and C, and about 11°C in case B (assuming turbulent boundary layers). The radiation term was therefore neglected when performing the step by step integration of equation (5). (In case B, Fig.15, the actual "final" temperature of the skin was about 360°K , on which the reduction to be expected from radiation would only be about 5°C).

Various conclusions can be drawn from Figs.14-17 as follows.

Effect of altitude

The effect of altitude on skin temperature is shown by comparing cases A and B (Figs.14 and 15). A missile at sea level reaches a higher temperature than its counterpart with a 45° trajectory although the flight speeds in cases A and B are little different for the first 20 seconds. In both cases an approximately steady temperature is reached after about 25 seconds.

Effect of heat capacity of skin

If the heat capacity of the skin is reduced by using a thinner gauge or a material with a lower specific heat, the transient temperature will increase at a more rapid rate. This is illustrated by a comparison of case A (Fig.14) in which the maximum temperature is reached in about 25 seconds and case C (Fig.16) with a corresponding time of 9 seconds. Both cases have similar flight histories but the more rapid temperature rise of the nose cone is in some part due to the increased heat transfer rate that occurs for flow over cones. It is interesting to note that for a skin with a low heat capacity the skin temperature curve approximates more nearly to the kinetic temperature curve so that the temperature fall is also more rapid as the missile decelerates.

The comparative heating effects of laminar and turbulent boundary layers

The considerable temperature reduction which can be obtained by maintaining a laminar layer over as large a range of Reynolds number as possible during the initial period of a flight is well illustrated in cases C and D (Figs.16 and 17).

3.2 Case involving a change of body geometry or transition

If it is necessary to deal with a change of body geometry such as a conical or ogival nose with a cylindrical afterbody then the calculation for each section should be performed separately. The ogive calculation will be similar to that described in the previous paragraph. The growth of the boundary layer from the tip to the rear of the ogive is different from its development along the cylinder and the value of k_H on the cylinder should be obtained as shown in Appendix VI. The effect of pressure gradients at the ogive-cylinder junction is ignored and the cylinder treated as a flat plate.

The procedure for calculation when transition is included is similar to that for a change of body geometry and temperature solutions must be made separately for the laminar and turbulent regions.

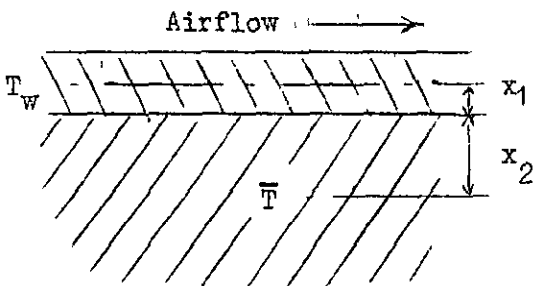
Both cases are considered in Appendix VI.

4 The determination of skin temperatures for a thin skin sandwich construction or for a single thin skin with heat loss to the interior

4.1 The calculation of transient temperatures in section 3 assumes that there is no heat loss from the inner surface of the skin. Some heat loss to the interior obviously does occur whether the outer skin is in contact with a supporting structure such as a second skin or whether it merely encloses an air space in an otherwise empty shell.

4.2 Numerical method

The problem of considering this heat loss is simplified as in the other transient cases if the calculation is based on average temperature only. The conditions for a double skin or a heated interior are therefore represented by those shown in the sketch.



T_w is the mean temperature of the outer skin, \bar{T} is the mean temperature of the inner skin or the interior and these mean values corresponding to planes positioned by x_1 and x_2 (e.g. the mid plane of a flat-plate).

Then in the notation of para.3

$$\frac{Q_1}{S} = c_{pw} \rho_1 g u_1 k_H (T_{wo} - T_w) \quad (7)$$

$$\frac{Q_2}{S} = \epsilon B T_w^4 \quad (8)$$

$$\frac{Q_3}{S} = G \frac{dT_w}{dt} \quad (9)$$

The heat transferred from the outer skin to the inner skin or the interior is

$$\frac{Q_4}{S} = (T_w - \bar{T}) \frac{1}{R} \quad (10)$$

where

$$R = \int_1^2 \frac{dx}{k} = \left(\frac{x_1}{k_1} + \frac{x_2}{k_2} \right) \quad (11)$$

(assuming a linear temperature gradient).

The heat balance for the outer skin is

$$G_1 \frac{dT_w}{dt} = c_{pw} \rho_1 g u_1 k_H (T_{wo} - T_w) - \epsilon B T_w^4 - (T_w - \bar{T}) \frac{1}{R} \quad (12)$$

Similarly the heat balance for the interior or inner skin is

$$G_2 \frac{d\bar{T}}{dt} = (T_w - \bar{T}) \frac{1}{R} \quad (13)$$

These simultaneous equations may be solved numerically⁴ giving T_w and \bar{T} as functions of time but the method is lengthy and is not presented here.

4.3 Approximate method

If however the variation of T_w with time is obtained by the numerical method (Appendices III, IV and V) for a single skin with no heat loss to the interior then an approximate estimate of the effect of such a loss can be made. If a linear approximation to the curve of T_w against time can be made and if it is assumed that the temperature space curve is continuous at the contact surface of the two media, then a relation between

\bar{T} , $(\bar{T})_{t=0}$, T_w and $\frac{\alpha t}{s^2}$ can be established¹⁰. This relation is shown in Fig.10 and is similar in form to that of the infinitely thick slab (Fig.11).

The two curves in Fig.10 are for an infinitely wide plate ($s =$ half the plate thickness) and for an infinitely long cylinder ($s =$ radius), the time t in the non dimension group $\frac{\alpha t}{s^2}$ correspond to a period over which T_w may be considered linear. The evaluation of $\alpha \left(\alpha = \frac{k}{\rho_s g c_s} \right)$ is straight in the case of a sandwich skin but if an air interior is considered then an equivalent coefficient of thermal conductivity k_e must be used to combine the effects of convection and conduction where k_e/k is a function of Grashof No. $\left(\frac{g \lambda \ell^3 \Delta T}{\nu^2} \right)$ (Ref.10) where λ is the coefficient of cubical expansion and ΔT a suitable temperature difference.

Two examples have been calculated on this basis:

(1) Case C (Fig.16) with heat transfer to the air interior of the cone.

An approximation to the temperature time curve was made and the decrease in skin temperature due to the internal heat loss was found to be less than 1°C for a flight time of 50 seconds.

(2) Case C (Fig.16) with heat transfer to an inner skin of cork.

A similar calculation indicates that the heat lost to a cork layer 0.40" thick attached to the inside surface of the fibre-glass would reduce the temperature of the fibre-glass by 2°C after 5 seconds and by 10°C after 50 seconds. The corresponding temperature rises of the cork are 10°C and 60°C.

5 The determination of temperature distribution in a skin of appreciable thickness
(Appendix VII for calculation method)

It is not possible to give an adequate treatment of this subject in this note, but a relatively simple theoretical case which has practical applications is presented in Appendix VII and Fig.11. This is the case of a semi infinite body with a constant initial temperature which has its surface temperature suddenly altered to and maintained at a new and constant value.

The semi infinite case may be applied in practice to castings, fairings, nose cones etc. of finite thickness without any great error until the temperature is such that appreciable heat transfer takes place at the second surface, provided the initial surface temperature rise is sufficiently rapid (e.g. case C).

Some typical time and depth limits for a given temperature to be exceeded are given for different materials in table IV. The effect of the ratio α (thermal conductivity/specific heat density) is such that the depth limit x is proportional to $(\alpha)^2$ whereas the time limit t varies inversely with α .

REFERENCES

<u>No.</u>	<u>Author</u>	<u>Title, etc.</u>
1	Keenan, J.H. Kaye, J.	Thermodynamic Properties of Air J. Wiley and Sons Ltd., 1945, New York
2	Kaye, G.W.C. Laby, F.H.	Physical and Chemical Constants Longmans, Green and Co., 1943 London, New York, Toronto
3	-	Tables of Supersonic Flow around Cones M.I.T. Technical Report No.1, 1947, Cambridge, Massachusetts
4	Piaggio, H.T.H.	An elementary treatise on Differential Equations and their applications G. Bell and Sons Ltd., 1948, London
5	Mangler, W.	Compressible Boundary Layers on Bodies of Revolution M.A.P. Volkenrode Ref. M.A.P. - VG 83, 1946
6	Monaghan, R. Johnson, J.E.	The measurement of heat transfer and skin friction at supersonic speeds Part II. Current Paper No.64 December, 1949
7	Monaghan, R.	An approximate solution of the com- pressible laminar boundary layer on a flat plate R. & M.2760 November, 1949
8	Nonweiler, T.	Rate of Heat Transfer due to Aerodynamic Heating at High Altitudes RAE Technical Note No. Aero 1834 ARC 10,578 December, 1946
9	Ingersoll, L.R. Zobell, O.J. Ingersoll, A.C.	Heat Conduction with engineering and geological applications McGraw-Hill Book Co., Inc., 1948 New York and London
10	Jakob, M.	Heat Transfer. Vol.1 John Wiley and Sons Ltd., 1949 New York
11	Young, A.D.	Skin friction in the laminar boundary layer in compressible flow ARC 11936 Cranfield Report No.20 July, 1948
12	-	Compressible Airflow Tables Oxford University Press (In preparation)

REFERENCES (Contd.)

<u>No.</u>	<u>Author</u>	<u>Title, etc.</u>
13	Squire, H.B.	Heat Transfer Calculations for Aerofoils R & M No.1986, November 1942
14	Stalder Jukoff	Heat Transfer to Bodies Travelling at High Speed in the Upper Atmosphere NACA Report 944, 1954

APPENDIX I

Stagnation and kinetic temperature rises

The stagnation temperature of a moving fluid is that attained when the flow is adiabatically brought to rest. Considering a stream tube, then the principle of conservation of energy gives the following relation between velocity and temperature

$$Jg \int_T^{T_H} c_p dT = \int_0^u u du \quad \text{I.1}$$

which if c_p is constant gives the well known formula

$$T_H - T = \frac{u^2}{2Jg c_p} \quad \text{I.2}$$

The stagnation temperature rise curve in Fig.4 has been evaluated from equation I.1, taking the integral

$$\int_T^{T_H} c_p dT$$

from Ref.1

If ΔT_{stag} is the temperature rise for a given velocity u , then the corresponding kinetic temperature rises are given by

$$\begin{aligned} \text{turbulent } \Delta T &= (P_r)^{1/3} \Delta T_{\text{stag}} \\ &\approx 0.90 \Delta T_{\text{stag}} \quad \text{when } P_r = 0.72 \end{aligned}$$

$$\begin{aligned} \text{laminar } \Delta T &= (P_r)^{1/2} \Delta T_{\text{stag}} \\ &\approx 0.85 \Delta T_{\text{stag}} \quad \text{when } P_r = 0.72 \end{aligned}$$

APPENDIX II

Derivation of aerodynamic heat transfer coefficients

Throughout this Report the heat transfer coefficient

$$k_H = \frac{Q_1/S}{\rho_1 u_1 g c_{PW} (T_{w_0} - T_{w\phi})} \quad \text{II.1}$$

is used and the values given in Fig.7 are taken from the latest experimental and theoretical evidence.

Fig.7 gives plots of

$$k_H \left(\frac{T_w}{T_1} \right)^n \text{ against } Re$$

where $n = 1/10$ for laminar layers

$n = 2.2/5$ for turbulent layers

and Re is Reynolds number $(u_1 \ell / \nu_1)$

The value of k_H is then obtained by multiplying $k_H \left(\frac{T_w}{T_1} \right)^n$ by the appropriate power of $\frac{T_1}{T_w}$ as given in Table VIII. The justification of this procedure is as follows.

(a) Laminar boundary layers

It can be shown that the formula

$$C_{FW} = 1.328 Re_w^{-1/2} \quad \text{II.2}$$

where subscript "w" denotes that density and viscosity are to be evaluated at skin temperature T_w , gives skin friction estimates for a flat plate within 5 per cent of those given by more accurate formulae (e.g. Young,¹¹) over the range covered by the present Report.

Accepting the relation

$$k_H = \frac{1}{2} C_F (P_r)^{-2/3} \quad \text{II.3}$$

we then obtain

$$k_{Hw} = 0.827 Re_w^{-1/2} \quad \text{II.4}$$

which, since

$$\frac{\rho_1}{\rho_w} = \frac{T_w}{T_1} \quad \text{II.5}$$

and taking

$$\frac{\mu_w}{\mu_1} = \left(\frac{T_w}{T_1} \right)^{0.8} \quad \text{II.6}$$

(which gives a fair mean for the temperature ranges involved) gives

$$k_H \left(\frac{T_w}{T_1} \right)^{1/10} = 0.827 \text{Re}^{-1/2} \quad \text{II.7}$$

which is the formula used in calculating the flat plate curve in Fig.7a.

The cone curve follows from the relation⁵

$$\frac{(k_H)_{\text{cone}}}{(k_H)_{\text{flat plate}}} = \frac{2}{\sqrt{3}} \quad \text{II.8}$$

(b) Turbulent boundary layers

Recent experimental evidence (unpublished) from R.A.E. tests has verified that the compressibility variation of k_H can be represented by a formula of the type proposed for skin friction in Ref.6. The formula for a flat plate is

$$k_{Hw} = 0.045 \left(\text{Re}_w \frac{T_1}{T_w} \right)^{-1/5} \quad \text{II.9}$$

which in terms of free stream conditions becomes

$$k_H \left(\frac{T_w}{T_1} \right)^{2.2/5} = 0.045 \text{Re}^{-1/5} \quad \text{II.10}$$

when

$$\frac{\mu_w}{\mu_1} = \left(\frac{T_w}{T_1} \right)^{0.8}$$

Furthermore the ratio of the zero heat transfer skin friction coefficients on cones and flat plates has been found to be $2/\sqrt{3}$ as for lamnar layers. Heat transfer coefficients have arbitrarily been assumed to bear the same relation, and from these formula the curves of Fig.7b have been produced.

APPENDIX III

A method of numerical integration

The differential equation to be solved for transient conditions over a thin skinned body is

$$\frac{dT_w}{dt} = \frac{c_{pw}}{G} \rho_1 g k_H u_1 (T_{wo} - T_w) - \frac{\epsilon B}{G} T_w^4 \quad \text{III.1}$$

If the radiation term is neglected this becomes

$$\frac{dT_w}{dt} = \frac{c_{pw}}{G} \rho_1 g k_H u_1 (T_{wo} - T_w) = f(t, T_w) \quad \text{III.2}$$

The method of numerical integration calculates a finite increment $\Delta T_w = (T_w)_{t=t_1} - (T_w)_{t=t_1-h}$ where h is a finite increment in t .

It can be shown that for the mid ordinate method⁴

$$\begin{aligned} (T_w)_{t=t_1} \approx & (T_w)_{t=t_1-h} + hf \left[t_1 - \frac{h}{2}, (T_w)_{t=t_1-h} \right. \\ & \left. + \frac{1}{2} hf \{ t_1 - h, (T_w)_{t=t_1-h} \} \right] \end{aligned} \quad \text{III.3}$$

If the initial conditions are known (i.e. at $t = 0$) a small increment h in t may be chosen, the 'inner' function $f_1 = f\{t_1-h, (T_w)_{t=t_1-h}\}$ and the 'outer' function $f_0 = f\{t_1-h/2, (T_w)_{t=t_1-h} + \frac{1}{2} hf_1\}$ can be evaluated, and a value of T_w obtained for the new value of t . This procedure may be repeated several times to any desired value of t and a solution found

$$T_w = f(t) \quad \text{III.4}$$

The layout of the calculations is given in Appendices IV and V.

APPENDIX IV

Calculation of transient temperatures for a wing or cylindrical body, using the integration method of Appendix III

The method of calculation is set out in Table V, and a numerical example is given in Table IX.

The initial condition $T_{w_{t=0}}$ and the flight history is known but for the sake of generalisation a subsequent value $T_{w_{n-2}}$ at t_{n-2} is taken. An increment h in t is chosen and a value $t_{n-1} = t_{n-2} + h$ inserted in column (1). The first row for each value of t is used to calculate the 'inner' function f_i and the second row to calculate the 'outer' function f_o (Appendix III). Column (3) contains the values of t and T_w to be used in calculating the function $f(t, T_w)$ in column (14).

The sequence of operations for the evaluation of the inner function is set out below.

Column	Operation
(4)	Ambient temperature. Read from Table I (Fig.1) in conjunction with the flight history.
(5)	Velocity. Read from flight history.
(6)	Kinetic temperature rise. Read from $\Delta T \sim$ velocity graph (Figs. 4b, c or d) using appropriate curve (laminar or turbulent).
(7)	(4) + (6)
(8)	c_{pw} from Fig.3 ρ_{og} is 0.0766 lb/ft ³ G from Table II (The values in Table II are for a skin thickness of one foot and must therefore be scaled down to the appropriate skin thickness).
(9)	(7) - $(T_w)_{n-2}$
(10)	Using $(T_1/T_w)_{n-2}$ read from Table VII.
(11)	To reduce time and labour the heat transfer coefficient $k_H (T_w/T_1)^{2.2/5}$ should be plotted against time t using the flight history graph, the Reynolds number velocity altitude nomogram (Fig.6) and the heat transfer coefficient Reynolds number graph (laminar or turbulent, Fig.7a or 7b); this may then be inserted in the Table at each step.
(12)	Read from Table I at the appropriate altitude.
(13)	This column is the same as (5) and is repeated for convenience in obtaining column (14).
(14)	(8) \times (9) \times (10) \times (11) \times (12) \times (13)
(15)	(14) \times $\frac{1}{2}h$
(16)	(15) + $(T_w)_{n-2}$

The value of (16) is then inserted in column (3) second row together with the time value $t_{n-1} - h/2$.

The outer function is then calculated in the second row with similar operations to those described above. The only difference is that columns (15) and (16) are unused, but instead we have

$$(17) \quad (14) \times h$$

$$(2) \quad (17) + (T_w)_{n-2}$$

This completes one step in the integration and further steps may be carried out until the desired time t or temperature T_w is reached.

Where the gradient $\frac{dT_w}{dt}$ is changing rapidly, for example during the initial stages of a flight, the time increment h should be smaller than that used during the later stages when $\frac{d^2T_w}{dt^2}$ is more nearly constant.

The suffices (e.g. $n-2$) refer to the time at which the terms are evaluated. Thus $(u_1)_{n-2}$ is the velocity just outside the boundary layer at a time $(t)_{n-2}$, where

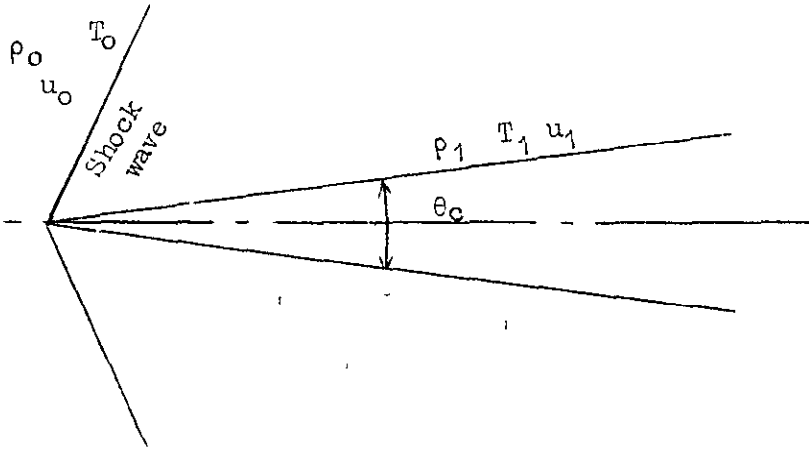
$$(t)_{n-2} = \sum_{j=1}^{j=n-2} h_j$$

from the commencement of the flight.

It should be noted that in certain cases it may be more convenient to group several columns together as one function and plot this against time before commencing the step by step process (e.g. columns (8), (11), (12) and (13) from Table V could be so grouped).

APPENDIX V

Calculation of transient skin temperatures for a
cone or ogive



The numerical integration process is little different from that for the flat plate described in Appendix IV except that the velocity temperature and density outside the boundary layer no longer have their ambient values (see sketch above).

To simplify the tabular operations (Table VI) the fundamental equation

$$G \frac{dT_w}{dt} = c_{pw} \rho_1 g u_1 k_H (T_{wo} - T_w) \quad V.1$$

has been rearranged to

$$\frac{dT_w}{dt} = \frac{c_{pw}}{\rho G} Re_\ell \mu_1 g k_H (T_{wo} - T_w) \quad V.2$$

The method of calculation is set out in Table VI. As in Table V the first row for each value of t is used to calculate the 'inner' function f_i and the second row to calculate the 'outer' function f_o (Appendix I). Column (3) contains the values of t and T_w to be used in calculating the function $f(t, T_w)$ in column (14).

The sequence of operations for the evaluation of the 'inner' function is set out below:

Column	Operation
(4)	Read from Fig.8a in conjunction with the flight history and Table I.
(5)	Read from Fig.8c in conjunction with the flight history.
(6)	Read from the $\Delta T \sim$ velocity graph (Figs.4b, 4c, 4d) laminar or turbulent curve as appropriate.
(7)	(4) + (6)

Column	Operation
(8)	Read from Fig.8b in conjunction with the flight history and Table I.
(9)	(5) repeated for convenience.
(10)	Read from Fig.2 in conjunction with T_1 .
(11)	(8) \times (9) \times appropriate length \div (10)
(12)	Read from Table VII using $(T_1/T_w)_{n-2}$
(13)	Cone : read from cone curve in Fig.7a or 7b Ogive: read from flat plate curve in Fig.7a or 7b and multiply by the appropriate value of β in Fig.9.
(14)	(7) - $(T_w)_{n-2}$
(15)	$\frac{c_{pw}}{\ell G}$ from Fig.3, Table II and using the appropriate length already used in column (11).
(16)	(10) \times (11) \times (12) \times (13) \times (14) \times (15)
(17)	(16) $\times \frac{1}{2}h$
(18)	$(T_w)_{n-2} + (17)$

The value of (18) is inserted in column (3) second row together with the time value $t_{n-1} - h/2$.

The 'outer' function is then calculated in the second row with similar operations to those described above. Two additional columns are required to complete the operation.

These are

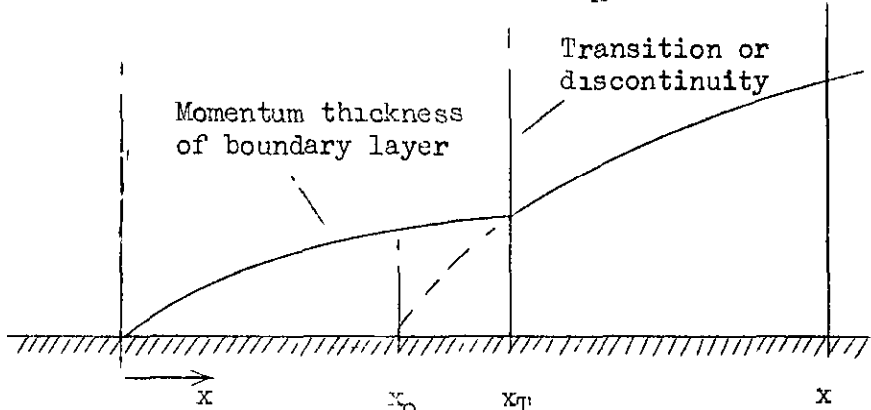
Column	Operation
(19)	(16) $\times h$
(20)	$(T_w)_{n-2} + (19)$

This completes one step in the integration and further steps may be carried out until the desired time t or temperature T_w is reached.

APPENDIX VI

Calculation of transient skin temperatures on a missile
with a discontinuity in the body geometry or a
boundary layer transition

The calculation must be performed separately for each section of continuity to allow for the variation of k_H



If the growth of a boundary layer in the transition region or near a discontinuity may be represented diagrammatically as shown then the calculation for $0 < x < x_T$ is as shown in Appendix IV or V.

The overall skin friction coefficient C_F on a flat plate is given by

$$C_{F_{x-x_T}} = 2 \frac{(\theta - \theta_T)}{x - x_T} \quad \text{VI.1}$$

where

$$2\theta = C_{F_{x-x_0}} (x - x_0) \quad \text{VI.2}$$

$$2\theta_T = C_{F_{x_T-x_0}} (x_T - x_0) \quad \text{VI.3}$$

thus

$$C_{F_{x-x_T}} = \frac{C_{F_{x-x_0}} (x - x_0) - C_{F_{x_T-x_0}} (x_T - x_0)}{(x - x_T)} \quad \text{VI.4}$$

or

$$k_{H_{x-x_T}} = \frac{k_{H_{x-x_0}} (Re_x - Re_{x_0}) - k_{H_{x_T-x_0}} (Re_{x_T} - Re_{x_0})}{(Re_x - Re_{x_T})} \quad \text{VI.5}$$

The relation between Re_{x_T} and Re_{x_0} can be obtained by identifying the values of θ at $x = x_T$.

$$\text{For a laminar layer } \theta = 0.664 \operatorname{Re}_{x_0}^{-1/2} x \quad \text{VI.6}$$

$$\text{turbulent layer } \theta = 0.037 \operatorname{Re}_{x-x_0}^{-1/5} (x-x_0) \left(\frac{T_1}{T_w}\right)^{0.4} \quad \text{VI.7}$$

at $x = x_T$

$$0.664 \operatorname{Re}_{x_T}^{-1/2} x_T = 0.037 \operatorname{Re}_{x_T-x_0}^{-1/5} (x_T-x_0) \left(\frac{T_1}{T_w}\right)^{0.4} \quad \text{VI.8}$$

$$18 \approx \operatorname{Re}_{x_T}^{1/2} \frac{(x_T-x_0)}{x_T} \operatorname{Re}_{x_T-x_0}^{-1/5} \left(\frac{T_1}{T_w}\right)^{0.4} \quad \text{VI.9}$$

$$18 \approx \operatorname{Re}_{x_T}^{-1/2} (\operatorname{Re}_{x_T} - \operatorname{Re}_{x_0})^{0.8} \left(\frac{T_1}{T_w}\right)^{0.4} \quad \text{VI.10}$$

The variation of $(\operatorname{Re}_{x_T} - \operatorname{Re}_{x_0})$ with Re_{x_T} is plotted in Fig.12 for varying $\left(\frac{T_1}{T_w}\right)$.

For a given value of x_T or Re_{x_T} and $\left(\frac{T_w}{T_1}\right)$, Re_{x_0} can be found from Fig.12 and $k_{H,x-x_T}$ may be evaluated from equation VI.5. The calculation then proceeds as shown in Appendix IV or V.

APPENDIX VII

The temperature distribution through a semi-infinite slab initially at temperature T_i when its surface temperature is suddenly raised to and maintained at a constant value T_{wo}

The conduction equation for one dimensional heat flow along the x axis with yz planes isothermals is

$$\frac{\partial T_p}{\partial t} = \alpha \frac{\partial^2 T_p}{\partial x^2} \quad \text{VII.1}$$

where

$$\alpha = \frac{k_s}{\rho_s c_s} \quad \text{VII.2}$$

The solution to this equation with the conditions outlined in the heading is

$$\frac{T_{wo} - T_p}{T_{wo} - T_i} = \frac{2}{\sqrt{\pi}} \int_0^{\frac{x}{2\sqrt{\alpha t}}} e^{-\zeta^2} d\zeta \quad (\text{Ref.9}) \quad \text{VII.3}$$

The variation of this probability integral with its upper limit

$\frac{x}{2\sqrt{\alpha t}}$ is shown in Fig.11. Choosing T_{wo} and T_i from external conditions and α from the material of the slab, T_p can be evaluated from the curve for values of x and t . Some typical solutions are shown in Table IV.

APPENDIX VIII

Sources of data used

<u>Parameter</u>	<u>Reference</u>	<u>Table</u> (from present report)	<u>Figure</u>
c_{pw}	1	-	3
μ_g	12	I	2
ν	12	I	-
σ	12	I	1
T_o	12	I	1
α	12	I	-
ϵ	8	III	-
k_s	9	II	-
c_s	9	II	-
$\rho_s g$	9	II	-
$\left. \begin{array}{l} \frac{T_1}{T_o} \\ \frac{\rho_1}{\rho_o} \\ \frac{u_1}{u_o} \end{array} \right\} \text{Cone relations}$	3	-	8a
	3	-	8b
	3	-	8c
β	5	-	9

The heat transfer coefficients for laminar and turbulent boundary layers on flat plates are obtained from the following: (cf. Appendix III).

$$\begin{aligned} (k_H)_{\text{lam}} &= \frac{1}{2} C_F Pr^{-2/3} \\ &= 0.827 Re_x^{-1/2} \left(\frac{T_1}{T_w} \right)^{1/10} \end{aligned}$$

$$(k_H)_{\text{turb}} = 0.045 Re_x^{-1/5} \left(\frac{T_1}{T_w} \right)^{2.2/5}$$

APPENDIX IX

The effect of the boundary layer character on heat transfer

The mechanism of flow close to a body in a fluid stream is such that over the fore-body the retarded layer is laminar in character and remains stable up to a region on the body at which a critical Reynolds number is reached. For Reynolds numbers greater than Re_{crit} instability within the layer gradually destroys its laminar form and eventually it becomes fully turbulent. The interchange of energy between strata in a layer is considerably greater if it is turbulent and the heat transfer rate is correspondingly higher.

Skin temperature is therefore dependent on the condition of the boundary layer and if the effect of transition is to be included in the calculation then some estimate of its position must be made.

The transition Reynolds number is affected by several factors including the heat transfer conditions at the surface and the surface finish of the body, also the prediction of transition from wind tunnel data is unreliable because of the effect of free stream turbulence.

Although some theoretical and experimental investigations of the effect of these factors on the stability of the laminar boundary layer have been made it is only possible to give the following pointers to the prediction of a transition Reynolds number for a particular set of conditions. The boundary layer flow is stabilised and transition Reynolds number increased by withdrawing heat from the fluid to the body; heat transferred from the body to the fluid has a destabilising effect. A roughened surface or steps at plating joints will tend to induce an earlier transition. A typical transition Reynolds number for free flight (under zero heat transfer conditions) may be taken as 8×10^6 .

TABLE I

Table of the standard atmosphere below 100,000 ft

$$\rho_{SL} = 0.0766 \text{ lb/ft}^3$$

$$a_{SL} = 1116 \text{ ft/sec.}$$

$h(\text{ft} \times 10^3)$	T°C	T°C ABS	$\frac{a}{a_{SL}}$	Relative density σ	$\mu\text{g} \times 10^5$ lb/ft sec	$v \times 10^4$ ft ² /sec.
0	15.00	288.00	1.0000	1.0000	1.204	1.57
1	13.02	286.02	0.9966	0.9711	1.198	1.61
2	11.04	284.04	0.9931	0.9428	1.191	1.65
3	9.06	282.06	0.9896	0.9151	1.185	1.69
4	7.08	280.08	0.9862	0.8881	1.179	1.73
5	5.10	278.10	0.9827	0.8617	1.169	1.77
6	3.12	276.12	0.9792	0.8359	1.162	1.82
7	1.14	274.14	0.9756	0.8107	1.156	1.86
8	-0.84	272.16	0.9721	0.7860	1.150	1.91
9	-2.82	270.18	0.9686	0.7620	1.143	1.96
10	-4.80	268.20	0.9650	0.7385	1.137	2.01
11	-6.78	266.22	0.9614	0.7156	1.130	2.06
12	-8.76	264.24	0.9579	0.6932	1.124	2.12
13	-10.74	262.26	0.9543	0.6714	1.117	2.17
14	-12.72	260.28	0.9507	0.6500	1.111	2.23
15	-14.70	258.30	0.9470	0.6293	1.104	2.29
16	-16.68	256.32	0.9434	0.6090	1.095	2.35
17	-18.66	254.34	0.9397	0.5892	1.088	2.41
18	-20.64	252.36	0.9361	0.5699	1.082	2.48
19	-22.62	250.38	0.9324	0.5511	1.075	2.55
20	-24.60	248.40	0.9287	0.5328	1.069	2.62
21	-26.58	246.42	0.9250	0.5150	1.063	2.69
22	-28.56	244.44	0.9213	0.4976	1.053	2.77
23	-30.54	242.46	0.9175	0.4807	1.047	2.84
24	-32.52	240.48	0.9138	0.4642	1.040	2.93
25	-34.50	238.50	0.9100	0.4481	1.034	3.01
26	-36.48	236.52	0.9062	0.4325	1.027	3.10
27	-38.46	234.54	0.9024	0.4173	1.018	3.19
28	-40.44	232.56	0.8986	0.4025	1.011	3.28
29	-42.42	230.58	0.8948	0.3881	1.005	3.38
30	-44.40	228.60	0.8909	0.3742	0.9982	3.48
31	-46.38	226.62	0.8871	0.3606	0.9885	3.59
32	-48.36	224.64	0.8832	0.3473	0.9821	3.69
33	-50.34	222.66	0.8793	0.3345	0.9757	3.81
34	-52.32	220.68	0.8754	0.3220	0.9692	3.93

TABLE I (Contd.)

$h(\text{ft} \times 10^3)$	$T^\circ\text{C}$	$T^\circ\text{C ABS}$	$\frac{a}{a_{SL}}$	Relative density σ	$\mu\text{g} \times 10^5$ lb/ft sec.	$\nu \times 10^4$ ft ² /sec.
35	-54.30	218.70	0.8714	0.3099	0.9596	4.05
36	-56.28	216.72	0.8675	0.2981	0.9531	4.18
37	-56.46	216.54	0.8671	0.2844	0.9531	4.37
38	-56.46	216.54	0.8671	0.2710	0.9531	4.59
39	-56.46	216.54	0.8671	0.2583	0.9531	4.82
40	-56.46	216.54	0.8671	0.2462	0.9531	5.05
41	-56.46	216.54	0.8671	0.2346	0.9531	5.30
42	-56.46	216.54	0.8671	0.2236	0.9531	5.56
43	-56.46	216.54	0.8671	0.2131	0.9531	5.84
44	-56.46	216.54	0.8671	0.2031	0.9531	6.12
45	-56.46	216.54	0.8671	0.1936	0.9531	6.43
46	-56.46	216.54	0.8671	0.1845	0.9531	6.74
47	-56.46	216.54	0.8671	0.1758	0.9531	7.07
48	-56.46	216.54	0.8671	0.1676	0.9531	7.42
49	-56.46	216.54	0.8671	0.1597	0.9531	7.79
50	-56.46	216.54	0.8671	0.1522	0.9531	8.17
51	-56.46	216.54	0.8671	0.1451	0.9531	8.57
52	-56.46	216.54	0.8671	0.1383	0.9531	9.00
53	-56.46	216.54	0.8671	0.1318	0.9531	9.44
54	-56.46	216.54	0.8671	0.1256	0.9531	9.90
55	-56.46	216.54	0.8671	0.1197	0.9531	10.39
56	-56.46	216.54	0.8671	0.1141	0.9531	10.90
57	-56.46	216.54	0.8671	0.1087	0.9531	11.44
58	-56.46	216.54	0.8671	0.1036	0.9531	12.00
59	-56.46	216.54	0.8671	0.0988	0.9531	12.59
60	-56.46	216.54	0.8671	0.0941	0.9531	13.21
61	-56.46	216.54	0.8671	0.0897	0.9531	13.87
62	-56.46	216.54	0.8671	0.0855	0.9531	14.55
63	-56.46	216.54	0.8671	0.0815	0.9531	15.26
64	-56.46	216.54	0.8671	0.0777	0.9531	16.02
65	-56.46	216.54	0.8671	0.0740	0.9531	16.80
66	-56.46	216.54	0.8671	0.0705	0.9531	17.63
67	-56.46	216.54	0.8671	0.0672	0.9531	18.50
68	-56.46	216.54	0.8671	0.0641	0.9531	19.41
69	-56.46	216.54	0.8671	0.0611	0.9531	20.37
70	-56.46	216.54	0.8671	0.0582	0.9531	21.37
71	-56.46	216.54	0.8671	0.0555	0.9531	22.42
72	-56.46	216.54	0.8671	0.0529	0.9531	23.53
73	-56.46	216.54	0.8671	0.0504	0.9531	24.69
74	-56.46	216.54	0.8671	0.0480	0.9531	25.90

TABLE I (Contd.)

$h(\text{ft} \times 10^3)$	$T^{\circ}\text{C}$	$T^{\circ}\text{C ABS}$	$\frac{a}{a_{\text{SL}}}$	Relative density σ	$\mu\text{g} \times 10^5$ lb/ft sec.	$\nu \times 10^4$ ft ² /sec.
75	-56.46	216.54	0.8671	0.0458	0.9531	27.18
76	-56.46	216.54	0.8671	0.0436	0.9531	28.52
77	-56.46	216.54	0.8671	0.0416	0.9531	29.92
78	-56.46	216.54	0.8671	0.0396	0.9531	31.39
79	-56.46	216.54	0.8671	0.0378	0.9531	32.94
80	-56.46	216.54	0.8671	0.0360	0.9531	34.56
81	-56.46	216.54	0.8671	0.0343	0.9531	36.26
82	-56.46	216.54	0.8671	0.0327	0.9531	38.05
83	-56.46	216.54	0.8671	0.0312	0.9531	39.92
84	-56.46	216.54	0.8671	0.0297	0.9531	41.89
85	-56.46	216.54	0.8671	0.0283	0.9531	43.95
86	-56.46	216.54	0.8671	0.0270	0.9531	46.12
87	-56.46	216.54	0.8671	0.0257	0.9531	48.39
88	-56.46	216.54	0.8671	0.0245	0.9531	50.77
89	-56.46	216.54	0.8671	0.0234	0.9531	53.27
90	-56.46	216.54	0.8671	0.0223	0.9531	55.89
91	-56.46	216.54	0.8671	0.0212	0.9531	58.65
92	-56.46	216.54	0.8671	0.0202	0.9531	61.53
93	-56.46	216.54	0.8671	0.0193	0.9531	64.56
94	-56.46	216.54	0.8671	0.0184	0.9531	67.74
95	-56.46	216.54	0.8671	0.0175	0.9531	71.08
96	-56.46	216.54	0.8671	0.0167	0.9531	74.58
97	-56.46	216.54	0.8671	0.0159	0.9531	78.25
98	-56.46	216.54	0.8671	0.0151	0.9531	82.10
99	-56.46	216.54	0.8671	0.0144	0.9531	86.15
100	-56.46	216.54	0.8671	0.0138	0.9531	90.39

TABLE II
Material properties

Material	Specific Heat c_s	Thermal conductivity k_s CHU/ft ² °C sec/ft	Weight ρ_s g lb/ft ³	G/ft	α
Aluminium	0.210	3.38×10^{-2}	168.5	35.4	9.55×10^{-4}
Magnesium	0.246	2.53×10^{-2}	108.6	26.7	9.48×10^{-4}
Steel (mild)	0.110	7.20×10^{-3}	487.0	53.6	1.34×10^{-4}
Nuron Fibre Glass	0.220	4.86×10^{-5}	115.3	25.4	1.92×10^{-6}
Polystyrene	0.32	1.278×10^{-5}	65.9	21.1	6.06×10^{-7}
Polythene	0.50	6.72×10^{-5}	58.6	29.3	2.30×10^{-6}
Perspex	0.35	3.03×10^{-5}	74.3	26.0	1.16×10^{-6}
Glass (Crown)	0.16	1.68×10^{-4}	150-162	24.0 -25.9	7.00×10^{-6} -6.48×10^{-6}
Glass (Flint)	0.12	1.34×10^{-4}	181-281	21.7 -33.7	6.17×10^{-6} -3.97×10^{-6}

TABLE III
Emmissivities and Absorptivities

Material	Emmissivity 100°F	ϵ 500°F	Absorptivity to Solar Radiation
Aluminium Polished	0.04	0.05	0.4*
Oxidised	0.11	0.12	0.2*
Steel Polished	0.07	0.10	0.4*
Carbonised	0.52	0.53	
Oxidised	0.79	0.79	0.2*
	100°F	750°F	
Lampblack paint	0.96	0.97	0.97
White paint	0.97	0.91	0.15

*Doubtful values

TABLE IV

Temperature time space distribution through a
semi infinite body

Material	Time for $\frac{T_{wo} - T_p}{T_{wo} - T_i} < 0.2$ for $0 < x < 0.1$ ft (secs)	Depth x throughout which $\frac{T_{wo} - T_p}{T_{wo} - T_i} < 0.2$ for $t = 60$ secs (INS)
Magnesium	77	1.06
I.C.I. Polythene	3.39×10^4	0.05
DOW Polystyrene	1.27×10^5	0.026

TABLE V

Numeric solution of the transient skin temperature equation for a turbulent boundary layer on a flat plate of thin aerofoil

(1)	(2)	(3)	(4)	(5)	(6)	(7)	(8)	(9)	(10)	(11)	(12)	(13)	(14)	(15)	(16)	(17)
t	T_w	t, T_w	T_1	u_1	ΔT	$T_{wo} = T_1 + \Delta T$	$\frac{c_{pw} \rho_0 \epsilon}{G}$	$T_{wo} - T_w$	$\left(\frac{T_1}{T_w}\right)^{2.2/5}$	$k_H \left(\frac{T_w}{T_1}\right)^{2.2/5}$	σ	u_1	$f(t, T_w)$	$\frac{1}{2} hf$	$T_w + \frac{1}{2} hf$	hf
t_0	$(T_w)_{t=0}$															
t_1	-	$t_0, (T_w)_0$	$(T_1)_0$	$(u_1)_0$	$(\Delta T)_0$	$(T_{wo})_0$	$\left(\frac{c_{pw} \rho_0 \epsilon}{G}\right)_0$	$(T_{wo} - T_w)_0$	$\left(\frac{T_1}{T_w}\right)_0^{2.2/5}$	$\left(k_H \frac{T_w}{T_1}\right)_0^{2.2/5}$	$(\sigma)_0$	$(u_1)_0$	$f(t, T_w)_0$	$(\frac{1}{2} hf)_0$	$(T_w)_0 + (\frac{1}{2} hf)_0$	-
	$(T_w)_1$	$t_1 - h/2, (T_w)_0 + (\frac{1}{2} hf)_0$	$(T_1)_{\frac{1}{2}}$	$(u_1)_{\frac{1}{2}}$	$(\Delta T)_{\frac{1}{2}}$	$(T_{wo})_{\frac{1}{2}}$	$\left(\frac{c_{pw} \rho_0 \epsilon}{G}\right)_{\frac{1}{2}}$	$(T_{wo} - T_w)_{\frac{1}{2}}$	$\left(\frac{T_1}{T_w}\right)_{\frac{1}{2}}^{2.2/5}$	$\left(k_H \frac{T_w}{T_1}\right)_{\frac{1}{2}}^{2.2/5}$	$(\sigma)_{\frac{1}{2}}$	$(u_1)_{\frac{1}{2}}$	$f(t, T_w)_{\frac{1}{2}}$	-	-	$(hf)_{\frac{1}{2}}$
t_{n-2}	$(T_w)_{n-2}$															
	-	$t_{n-2}, (T_w)_{n-2}$	$(T_1)_{n-2}$	$(u_1)_{n-2}$	$(\Delta T)_{n-2}$	$(T_{wo})_{n-2}$	$\left(\frac{c_{pw} \rho_0 \epsilon}{G}\right)_{n-2}$	$(T_{wo} - T_w)_{n-2}$	$\left(\frac{T_1}{T_w}\right)_{n-2}^{2.2/5}$	$\left(k_H \frac{T_w}{T_1}\right)_{n-2}^{2.2/5}$	$(\sigma)_{n-2}$	$(u_1)_{n-2}$	$f(t, T_w)_{n-2}$	$(\frac{1}{2} hf)_{n-2}$	$(T_w)_{n-2} + (\frac{1}{2} hf)_{n-2}$	-
t_{n-1}	$(T_w)_{n-1}$	$t_{n-1} - h/2, (T_w)_{n-2} + (\frac{1}{2} hf)_{n-2}$	$(T_1)_{n-1}$	$(u_1)_{n-1}$	$(\Delta T)_{n-1}$	$(T_{wo})_{n-1}$	$\left(\frac{c_{pw} \rho_0 \epsilon}{G}\right)_{n-1}$	$(T_{wo} - T_w)_{n-1}$	$\left(\frac{T_1}{T_w}\right)_{n-1}^{2.2/5}$	$\left(k_H \frac{T_w}{T_1}\right)_{n-1}^{2.2/5}$	$(\sigma)_{n-1}$	$(u_1)_{n-1}$	$f(t, T_w)_{n-1}$	-	-	$(hf)_{n-1}$
	-	$t_{n-1}, (T_w)_{n-1}$	$(T_1)_{n-1}$	$(u_1)_{n-1}$	$(\Delta T)_{n-1}$	$(T_{wo})_{n-1}$	$\left(\frac{c_{pw} \rho_0 \epsilon}{G}\right)_{n-1}$	$(T_{wo} - T_w)_{n-1}$	$\left(\frac{T_1}{T_w}\right)_{n-1}^{2.2/5}$	$\left(k_H \frac{T_w}{T_1}\right)_{n-1}^{2.2/5}$	$(\sigma)_{n-1}$	$(u_1)_{n-1}$	$f(t, T_w)_{n-1}$	$(\frac{1}{2} hf)_{n-1}$	$(T_w)_{n-1} + (\frac{1}{2} hf)_{n-1}$	-
t_n	$(T_w)_n$	$t_n - h/2, (T_w)_{n-1} + (\frac{1}{2} hf)_{n-1}$	$(T_1)_n$	$(u_1)_n$	$(\Delta T)_n$	$(T_{wo})_n$	$\left(\frac{c_{pw} \rho_0 \epsilon}{G}\right)_n$	$(T_{wo} - T_w)_n$	$\left(\frac{T_1}{T_w}\right)_n^{2.2/5}$	$\left(k_H \frac{T_w}{T_1}\right)_n^{2.2/5}$	$(\sigma)_n$	$(u_1)_n$	$f(t, T_w)_n$	-	-	$(hf)_n$

TABLE VI

Numerical solution of the transient skin temperature equation for a turbulent boundary layer on a conical or ogival body

(1)	(2)	(3)	(4)	(5)	(6)	(7)	(8)	(9)	(10)	(11)	(12)	(13)	(14)	(15)	(16)	(17)	(18)	(19)
t	T_w	t, T_w	T_1	u_1	ΔT	$T_{wo} = T_1 + \Delta T$	$\rho_1 g$	u_1	$\mu_1 g$	$Re\ell$	$\left(\frac{T_1}{T_w}\right)^{\frac{2.2}{5}}$	$k_H \left(\frac{T_w}{T_1}\right)^{\frac{2.2}{5}}$	$T_{wo} - T_w$	$\frac{c_{pw}}{\ell G}$	$f(t, T_w)$	$\frac{1}{2} hf$	$T_w + \frac{1}{2} hf$	hf
t_0	$(T_w)_{t=0}$																	
t_1	-	$t_0, (T_w)_0$	$(T_1)_0$	$(u_1)_0$	$(\Delta T)_0$	$(T_{wo})_0$	$(\rho_1 g)_0$	$(u_1)_0$	$(\mu_1 g)_0$	$(Re\ell)_0$	$\left(\frac{T_1}{T_w}\right)^{\frac{2.2}{5}}$	$\left(k_H \left(\frac{T_w}{T_1}\right)^{\frac{2.2}{5}}\right)_0$	$(T_{wo} - T_w)_0$	$\left(\frac{c_{pw}}{\ell G}\right)_0$	$f(t, T_w)_0$	$(\frac{1}{2} hf)_0$	$(T_w)_0 + (\frac{1}{2} hf)_0$	-
	$(T_w)_1$	$t_1 - h/2,$ $(T_w)_0 + (\frac{1}{2} hf)_0$	$(T_1)_{\frac{1}{2}}$	$(u_1)_{\frac{1}{2}}$	$(\Delta T)_{\frac{1}{2}}$	$(T_{wo})_{\frac{1}{2}}$	$(\rho_1 g)_{\frac{1}{2}}$	$(u_1)_{\frac{1}{2}}$	$(\mu_1 g)_{\frac{1}{2}}$	$(Re\ell)_{\frac{1}{2}}$	$\left(\frac{T_1}{T_w}\right)^{\frac{2.2}{5}}$	$\left(k_H \left(\frac{T_w}{T_1}\right)^{\frac{2.2}{5}}\right)_{\frac{1}{2}}$	$(T_{wo} - T_w)_{\frac{1}{2}}$	$\left(\frac{c_{pw}}{\ell G}\right)_{\frac{1}{2}}$	$f(t, T_w)_{\frac{1}{2}}$	-	-	$(hf)_{\frac{1}{2}}$
t_{n-2}	$(T_w)_{n-2}$																	
t_{n-1}	-	$t_{n-2},$ $(T_w)_{n-2}$	$(T_1)_{n-2}$	$(u_1)_{n-2}$	$(\Delta T)_{n-2}$	$(T_{wo})_{n-2}$	$(\rho_1 g)_{n-2}$	$(u_1)_{n-2}$	$(\mu_1 g)_{n-2}$	$(Re\ell)_{n-2}$	$\left(\frac{T_1}{T_w}\right)^{\frac{2.2}{5}}$	$\left(k_H \frac{T_w}{T_1}\right)_{n-2}$	$(T_{wo} - T_w)_{n-2}$	$\left(\frac{c_{pw}}{\ell G}\right)_{n-2}$	$f(t, T_w)_{n-2}$	$(\frac{1}{2} hf)_{n-2}$	$(T_w)_{n-2} + (\frac{1}{2} hf)_{n-2}$	-
	$(T_w)_{n-1}$	$t_{n-1} - h/2,$ $(T_w)_{n-2} + (\frac{1}{2} hf)_{n-2}$	$(T_1)_{n-1\frac{1}{2}}$	$(u_1)_{n-1\frac{1}{2}}$	$(\Delta T)_{n-1\frac{1}{2}}$	$(T_{wo})_{n-1\frac{1}{2}}$	$(\rho_1 g)_{n-1\frac{1}{2}}$	$(u_1)_{n-1\frac{1}{2}}$	$(\mu_1 g)_{n-1\frac{1}{2}}$	$(Re\ell)_{n-1\frac{1}{2}}$	$\left(\frac{T_1}{T_w}\right)^{\frac{2.2}{5}}$	$\left(k_H \frac{T_w}{T_1}\right)_{n-1\frac{1}{2}}$	$(T_{wo} - T_w)_{n-1\frac{1}{2}}$	$\left(\frac{c_{pw}}{\ell G}\right)_{n-1\frac{1}{2}}$	$f(t, T_w)_{n-1\frac{1}{2}}$	-	-	$(hf)_{n-1\frac{1}{2}}$
t_n	-	$t_{n-1},$ $(T_w)_{n-1}$	$(T_1)_{n-1}$	$(u_1)_{n-1}$	$(\Delta T)_{n-1}$	$(T_{wo})_{n-1}$	$(\rho_1 g)_{n-1}$	$(u_1)_{n-1}$	$(\mu_1 g)_{n-1}$	$(Re\ell)_{n-1}$	$\left(\frac{T_1}{T_w}\right)^{\frac{2.2}{5}}$	$\left(k_H \frac{T_w}{T_1}\right)_{n-1}$	$(T_{wo} - T_w)_{n-1}$	$\left(\frac{c_{pw}}{\ell G}\right)_{n-1}$	$f(t, T_w)_{n-1}$	$(\frac{1}{2} hf)_{n-1}$	$(T_w)_{n-1} + (\frac{1}{2} hf)_{n-1}$	-
	$(T_w)_n$	$t_n - h/2,$ $(T_w)_{n-1} + (\frac{1}{2} hf)_{n-1}$	$(T_1)_{n-\frac{1}{2}}$	$(u_1)_{n-\frac{1}{2}}$	$(\Delta T)_{n-\frac{1}{2}}$	$(T_{wo})_{n-\frac{1}{2}}$	$(\rho_1 g)_{n-\frac{1}{2}}$	$(u_1)_{n-\frac{1}{2}}$	$(\mu_1 g)_{n-\frac{1}{2}}$	$(Re\ell)_{n-\frac{1}{2}}$	$\left(\frac{T_1}{T_w}\right)^{\frac{2.2}{5}}$	$\left(k_H \frac{T_w}{T_1}\right)_{n-\frac{1}{2}}$	$(T_{wo} - T_w)_{n-\frac{1}{2}}$	$\left(\frac{c_{pw}}{\ell G}\right)_{n-\frac{1}{2}}$	$f(t, T_w)_{n-\frac{1}{2}}$	-	-	$(hf)_{n-\frac{1}{2}}$

TABLE VII

Values of $\left(\frac{T_1}{T_w}\right)^{\frac{2.2}{5}}$ and $\left(\frac{T_1}{T_w}\right)^{\frac{1}{10}}$

$\frac{T_1}{T_w}$	$\left(\frac{T_1}{T_w}\right)^{\frac{2.2}{5}}$	$\left(\frac{T_1}{T_w}\right)^{\frac{1}{10}}$	$\frac{T_1}{T_w}$	$\left(\frac{T_1}{T_w}\right)^{\frac{2.2}{5}}$	$\left(\frac{T_1}{T_w}\right)^{\frac{1}{10}}$
0.30	0.5887	0.8866	0.65	0.8273	0.9578
0.31	0.5973	0.8895	0.66	0.8329	0.9593
0.32	0.6057	0.8923	0.67	0.8384	0.9607
0.33	0.6140	0.8951	0.68	0.8439	0.9622
0.34	0.6221	0.8977	0.69	0.8494	0.9636
0.35	0.6301	0.9003	0.70	0.8548	0.9650
0.36	0.6379	0.9029	0.71	0.8601	0.9663
0.37	0.6457	0.9054	0.72	0.8654	0.9677
0.38	0.6533	0.9078	0.73	0.8707	0.9690
0.39	0.6608	0.9101	0.74	0.8759	0.9703
0.40	0.6682	0.9124	0.75	0.8811	0.9716
0.41	0.6755	0.9147	0.76	0.8863	0.9729
0.42	0.6827	0.9169	0.77	0.8914	0.9742
0.43	0.6898	0.9191	0.78	0.8964	0.9755
0.44	0.6968	0.9212	0.79	0.9015	0.9767
0.45	0.7037	0.9233	0.80	0.9065	0.9779
0.46	0.7106	0.9253	0.81	0.9115	0.9791
0.47	0.7173	0.9273	0.82	0.9164	0.9803
0.48	0.7240	0.9292	0.83	0.9213	0.9815
0.49	0.7306	0.9311	0.84	0.9261	0.9827
0.50	0.7371	0.9330	0.85	0.9310	0.9839
0.51	0.7436	0.9349	0.86	0.9358	0.9850
0.52	0.7500	0.9367	0.87	0.9406	0.9862
0.53	0.7563	0.9385	0.88	0.9453	0.9873
0.54	0.7625	0.9402	0.89	0.9500	0.9884
0.55	0.7687	0.9420	0.90	0.9547	0.9895
0.56	0.7748	0.9437	0.91	0.9593	0.9906
0.57	0.7809	0.9453	0.92	0.9640	0.9917
0.58	0.7869	0.9470	0.93	0.9686	0.9928
0.59	0.7928	0.9486	0.94	0.9731	0.9938
0.60	0.7987	0.9502	0.95	0.9777	0.9949
0.61	0.8045	0.9518	0.96	0.9822	0.9959
0.62	0.8103	0.9533	0.97	0.9867	0.9970
0.63	0.8160	0.9548	0.98	0.9912	0.9980
0.64	0.8217	0.9564	0.99	0.9956	0.9990
0.65	0.8273	0.9578	1.00	1.00	1.00

TABLE VIII

Example Numerical solution ($0 < t < 6$) of the transient skin temperatures of a thin acrofoil with a turbulent boundary layer (Case A)

(1)	(2)	(3)	(4)	(5)	(6)	(7)	(8)	(9)	(10)	(11)	(12)	(13)	(14)	(15)	(16)	(17)
t	T_w	t, T_w	T_1	u_1	ΔT	$T_{wo} = T_1 + \Delta T$	$\frac{c_{pw} \rho_o g}{G}$	$T_{wo} - T_w$	$\left(\frac{T_1}{T_w}\right)^{\frac{2.2}{5}}$	$k_H \left(\frac{T_w}{T_1}\right)^{\frac{2.2}{5}}$	σ	u_1	$f(t, T_w)$	$\frac{1}{2}hf$	$T_w + \frac{1}{2}hf$	hf
0	288															
1		0.288	288	0	0	288	0.0383	0	1.0	0	1.0	0	0	0	288	
	288.119	$\frac{1}{2}, 288$	^	342	5.0	293	^	5.0	1.0	1.82	^	342	0.119			0.119
1.5		1, 288.12		683	20.0	308		19.88	0.9998	1.60		683	0.832	0.208	288.33	
	288.86	1.25, 288.33		854	30.0	318		29.67	0.9995	1.53		854	1.484			0.742
2.0		1.5, 288.86		1025	43.2	331		42.34	0.9987	1.455		1025	2.415	0.604	289.46	
	290.74	1.75, 289.46		1195	59.5	347.5		58.04	0.9978	1.42		1195	3.764			1.882
2.5		2.0, 290.74		1366	77.5	365.5		74.76	0.9958	1.38		1366	5.375	1.344	292.08	
	294.39	2.25, 292.08		1537	98	386		93.92	0.9938	1.33		1537	7.308			3.654
3.0		2.5, 294.39		1708	121	409		114.61	0.9904	1.31		1708	9.727	2.432	296.82	
	300.56	2.75, 296.82		1878	145.6	433.6		136.78	0.9868	1.27		1878	12.33			6.165
4.0		3.0, 300.56		2049	172.8	460.8		160.24	0.9814	1.26		2049	15.55	7.775	308.34	
	315.05	3.5, 308.34		2040	172	460.0		151.66	0.9704	1.26		2040	14.49			14.49
5.0		4.0, 315.05		2030	170	458		142.95	0.9620	1.261		2030	13.483	6.742	321.79	
	327.56	4.5, 321.79		2020	168.4	456.4		134.61	0.9514	1.263		2020	12.514			12.514
6.0		5.0, 327.56	v	2010	167.0	455		127.44	0.9449	1.265	v	2010	11.727	5.864	333.42	
	338.44	5.5, 333.42	v	2000	165.0	453		119.58	0.9376	1.267	v	2000	10.881			10.881

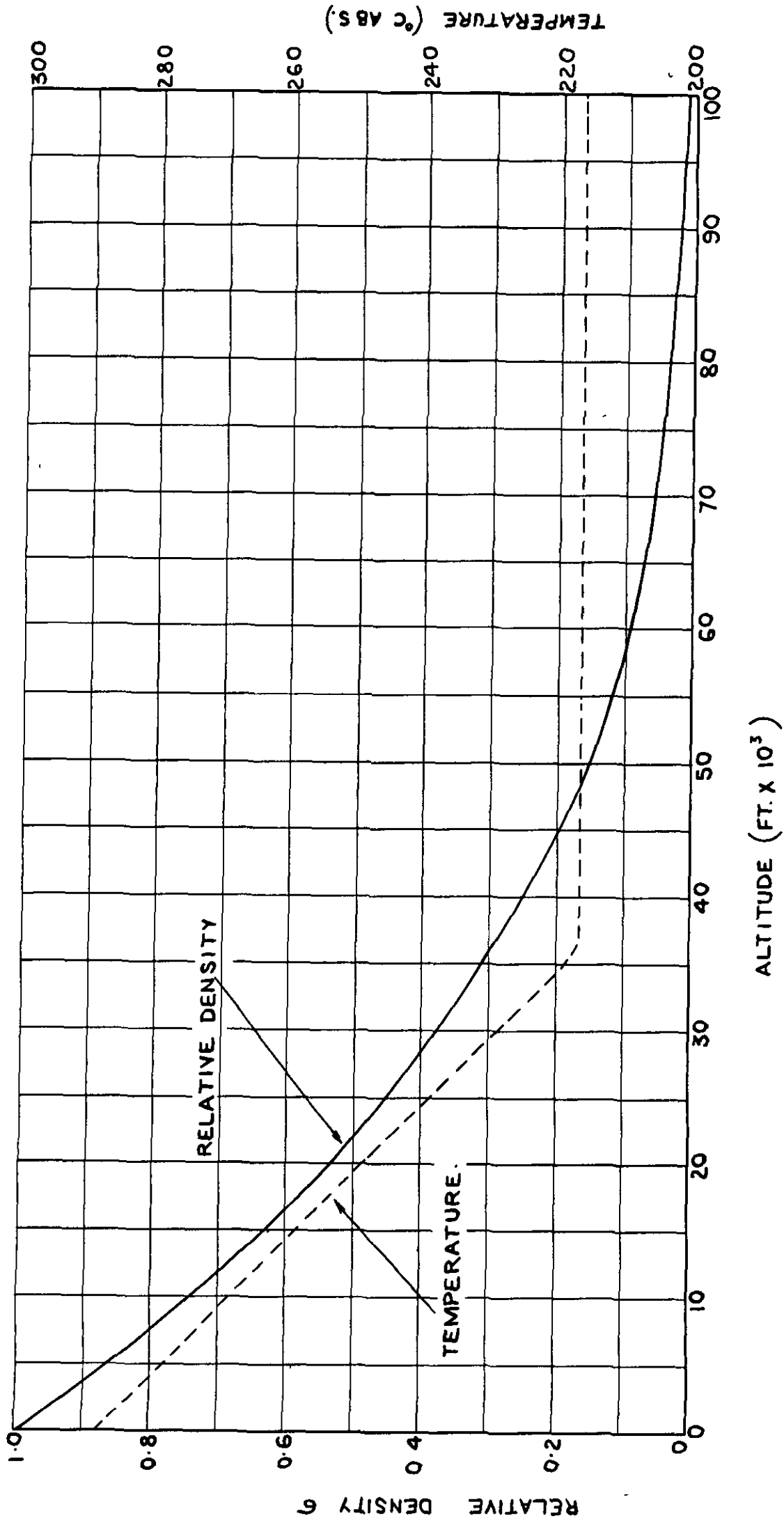


FIG. I. STANDARD ATMOSPHERE CURVES.

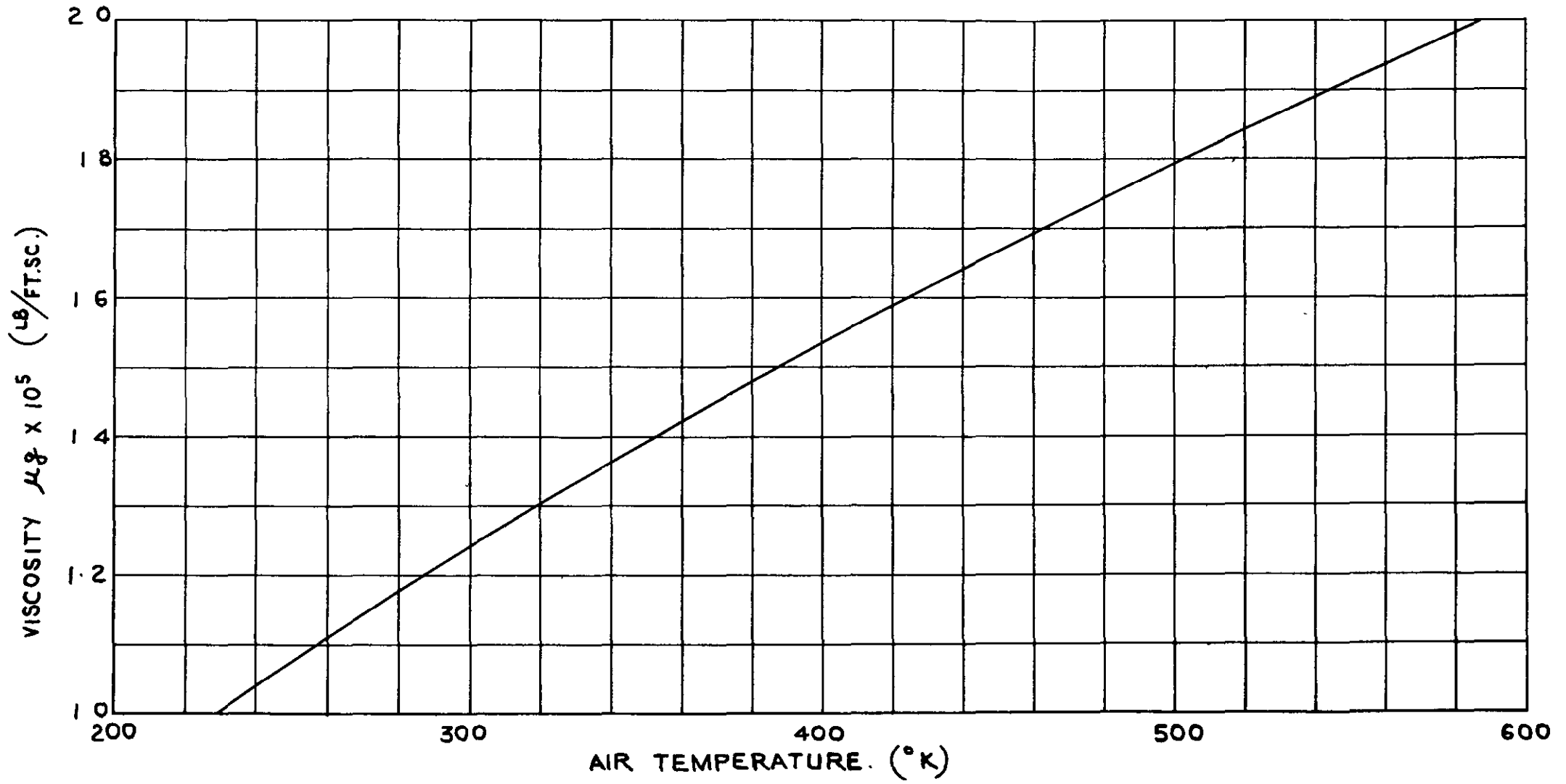


FIG.2. VARIATION OF VISCOSITY OF AIR WITH TEMPERATURE.
 (ASSUMING SUTHERLAND'S FORMULA WITH $T_c = 114^\circ\text{K}$ AND $\mu_{g,273} = 1.15 \times 10^{-5}$ LB/FT.SC)

FIG. 3.

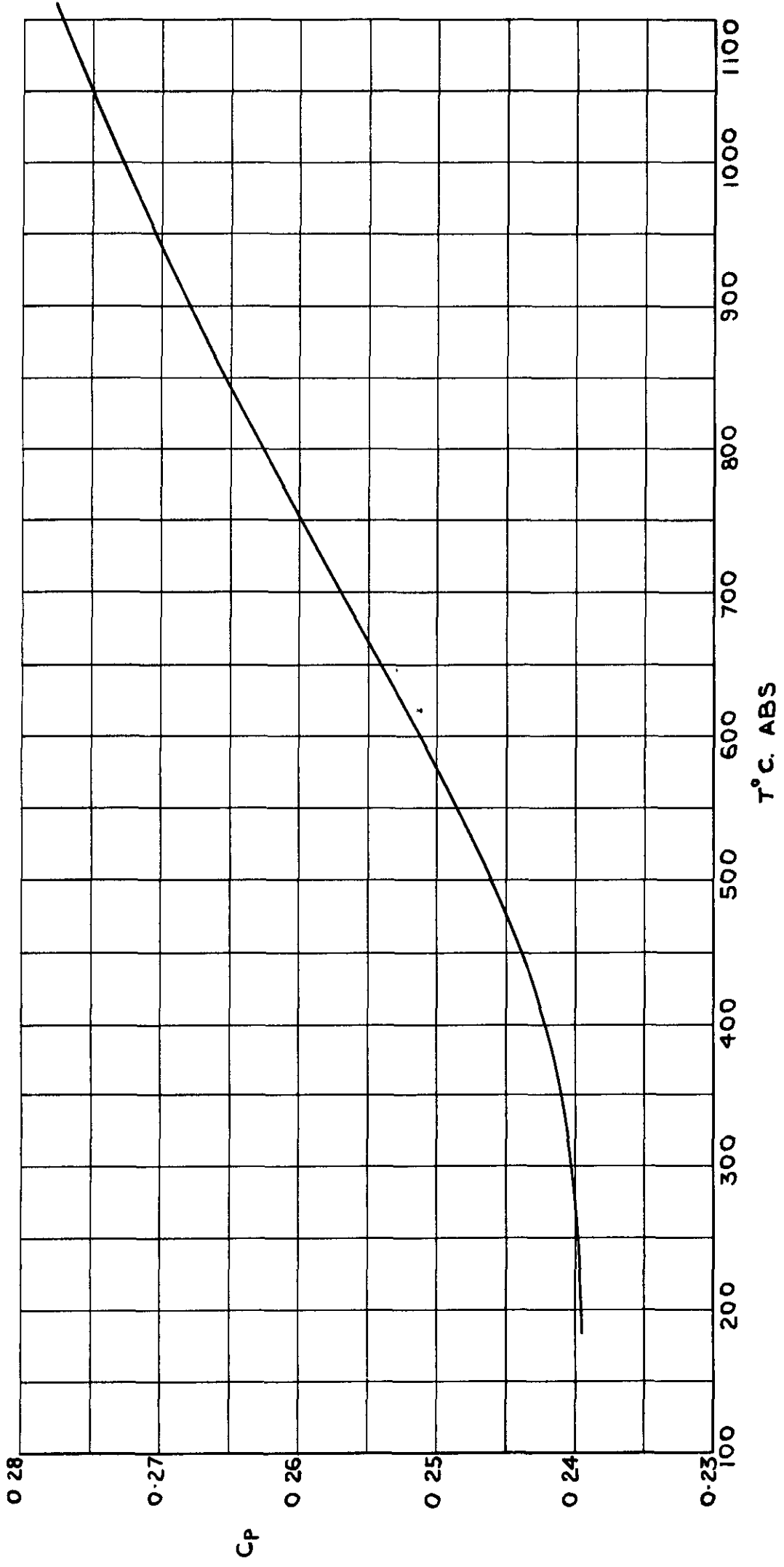


FIG. 3. VARIATION WITH TEMPERATURE OF THE SPECIFIC HEAT OF AIR AT CONSTANT PRESSURE.

FIG.4.a.

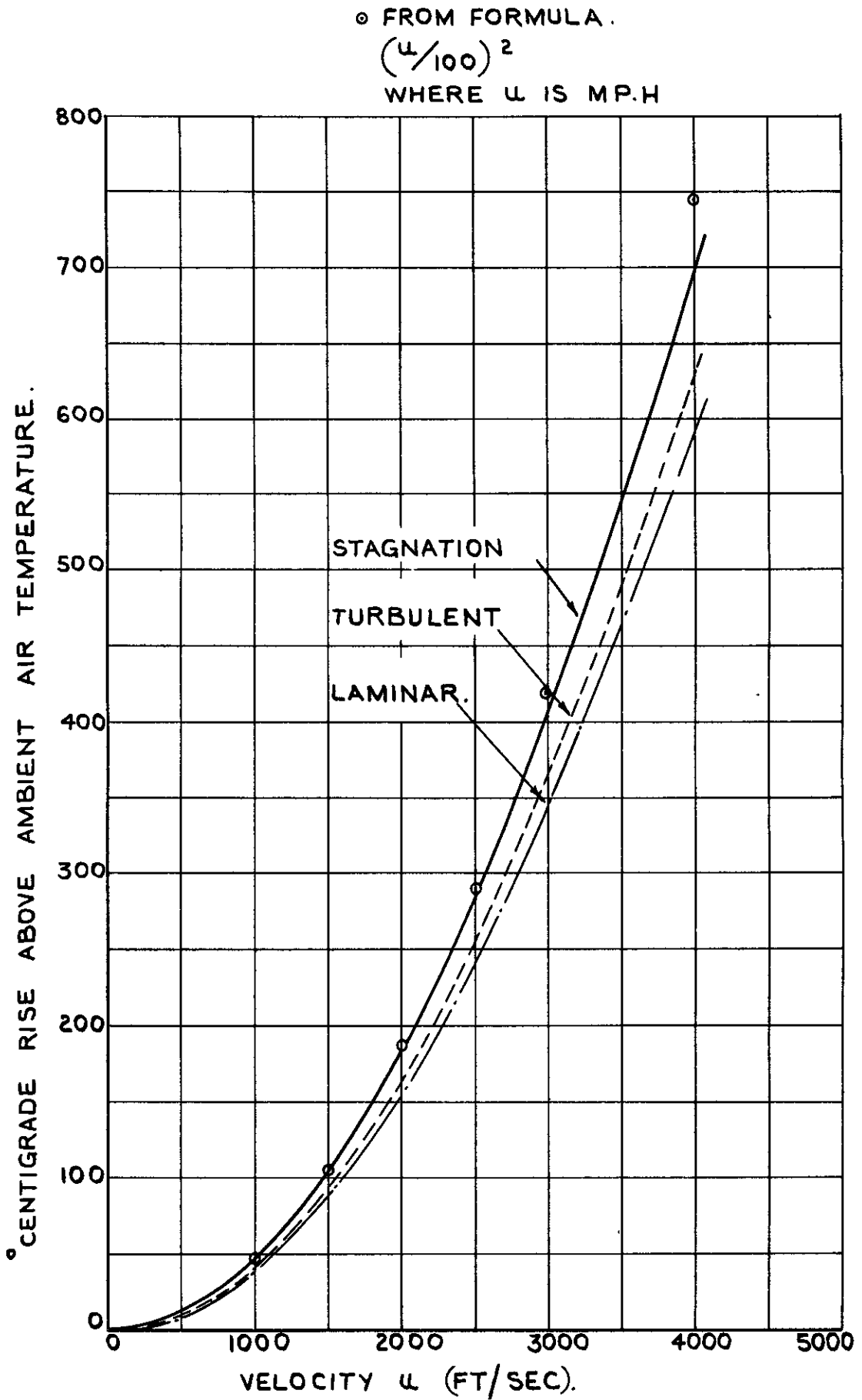


FIG.4.a. STAGNATION & KINETIC TEMPERATURE RISES (VARIABLE C_p)

FIG. 4 b

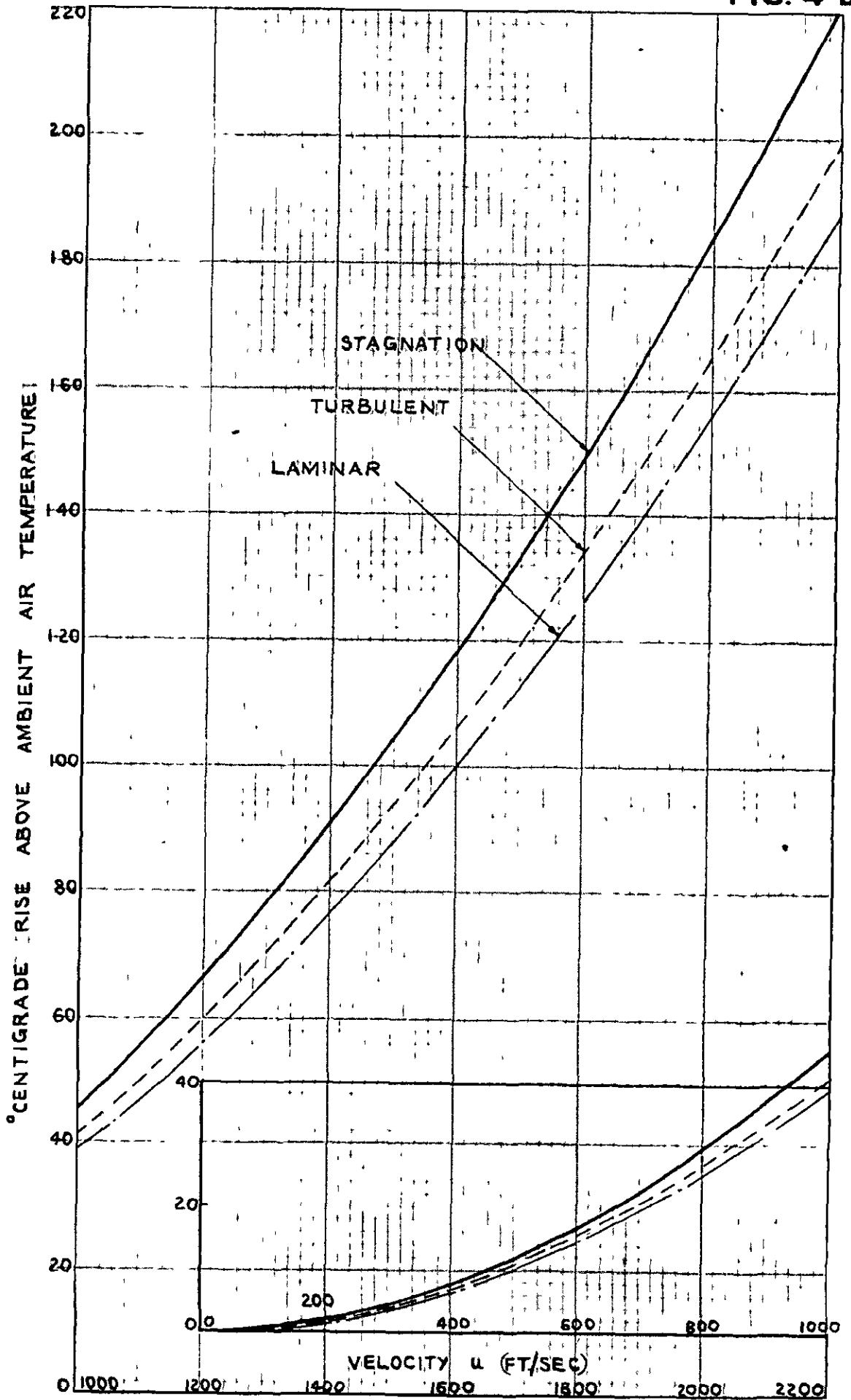


FIG.4b STAGNATION AND KINETIC TEMPERATURE RISES (VARIABLE C_p)

FIG. 4 c

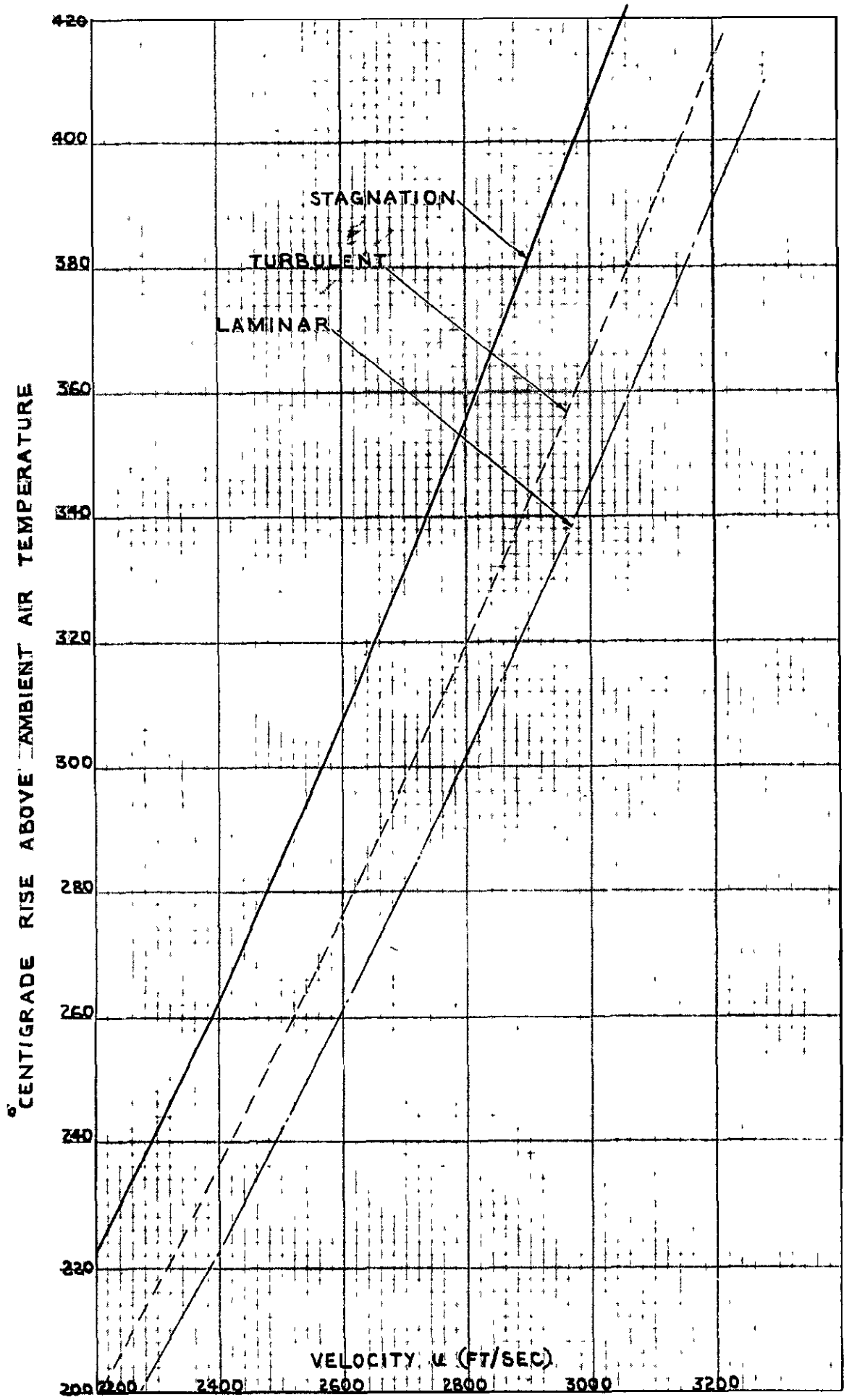


FIG. 4 c STAGNATION AND KINETIC TEMPERATURE RISES! (VARIABLE C_p)

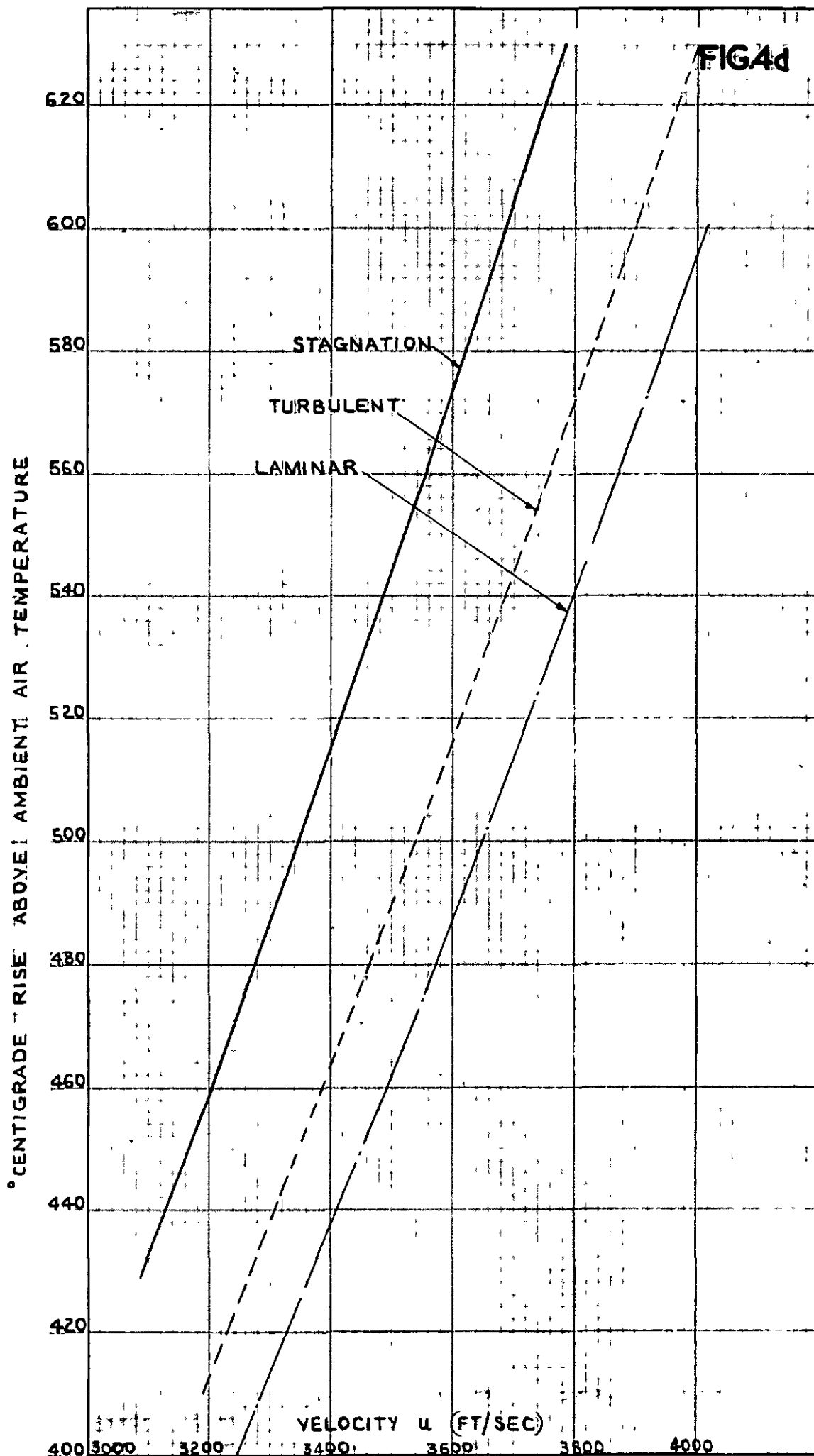


FIG 4d STAGNATION AND KINETIC TEMPERATURE RISES (VARIABLE C_p)

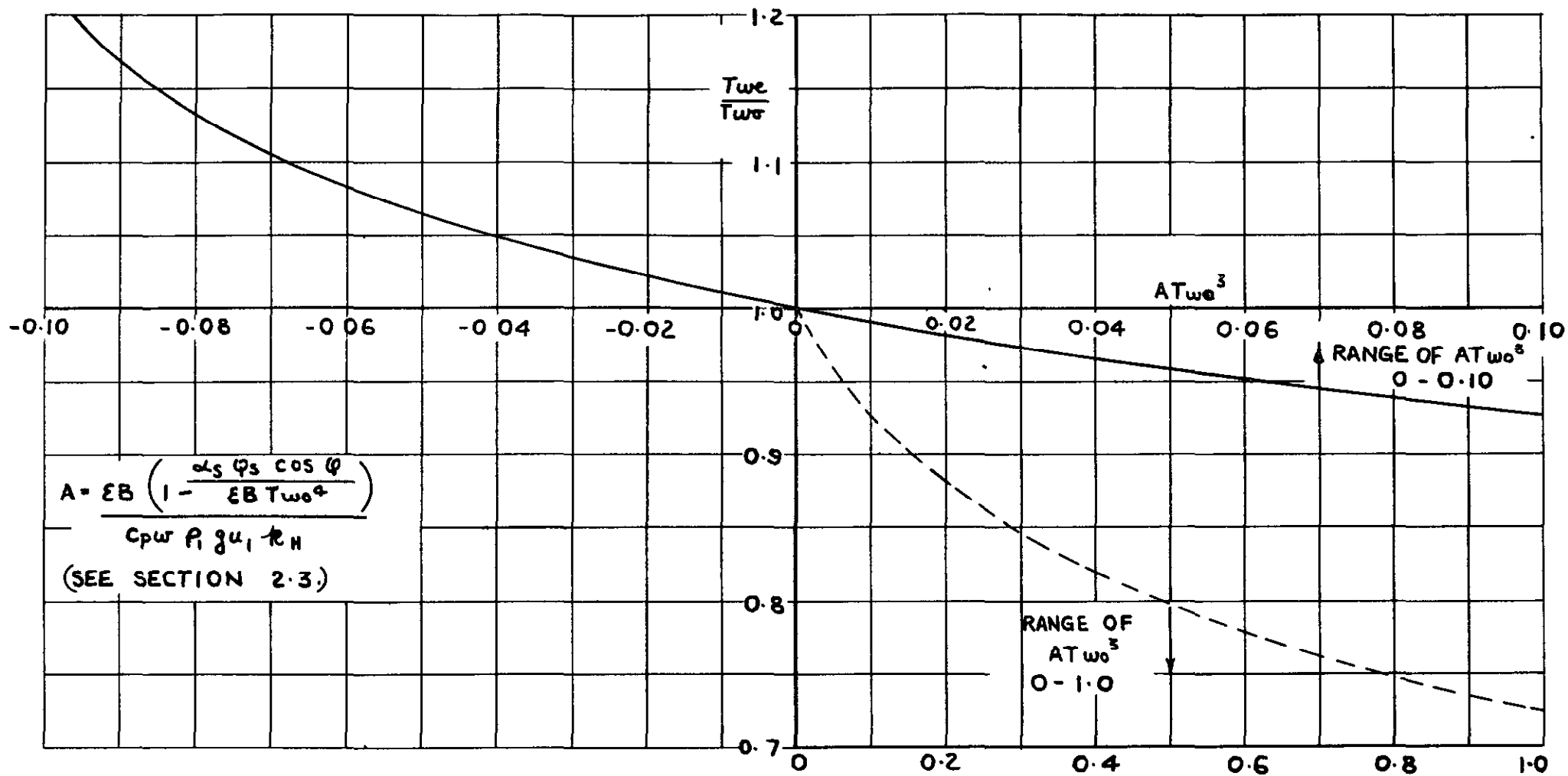


FIG 5. APPROXIMATE DETERMINATION OF EQUILIBRIUM TEMPERATURE.

T_w = KINETIC TEMPERATURE.

T_w^e = EQUILIBRIUM TEMPERATURE

FIG. 6.

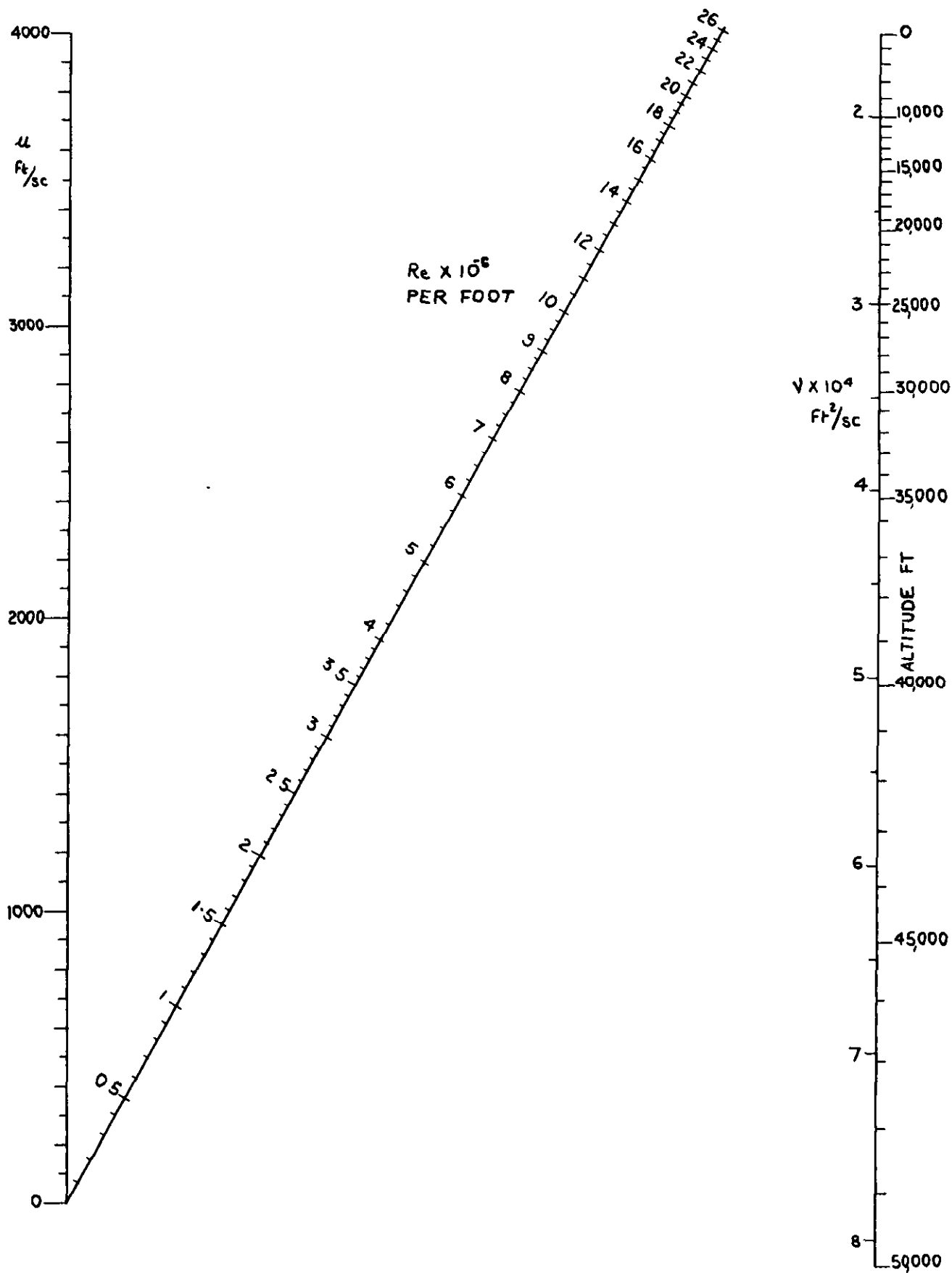


FIG. 6. NOMOGRAM GIVING VARIATION OF REYNOLDS NUMBER PER FOOT WITH SPEED & HEIGHT.

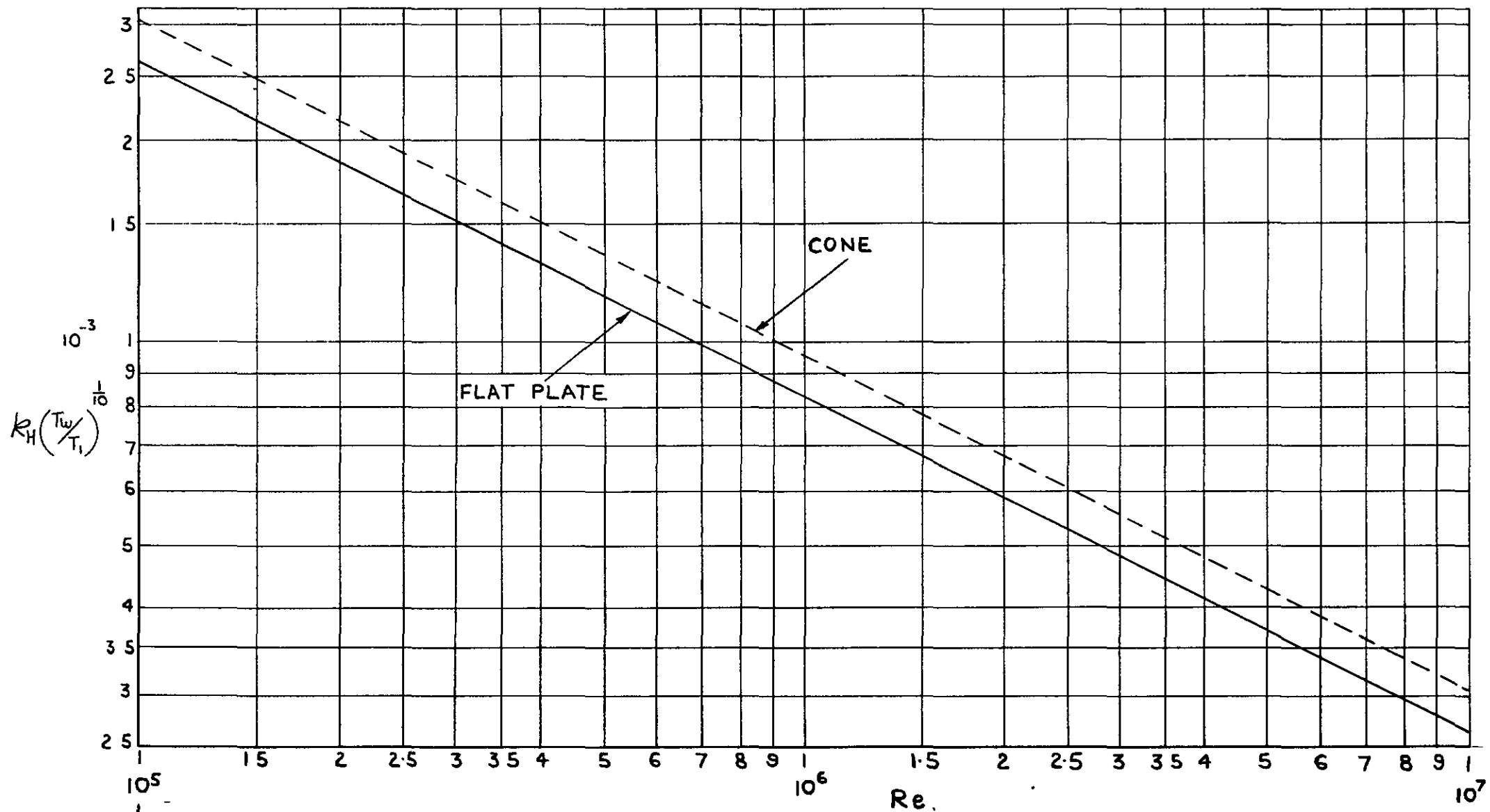


FIG. 7a. HEAT TRANSFER COEFFICIENTS FOR THE LAMINAR BOUNDARY LAYER.

10^{-4}

FIG 7.b.

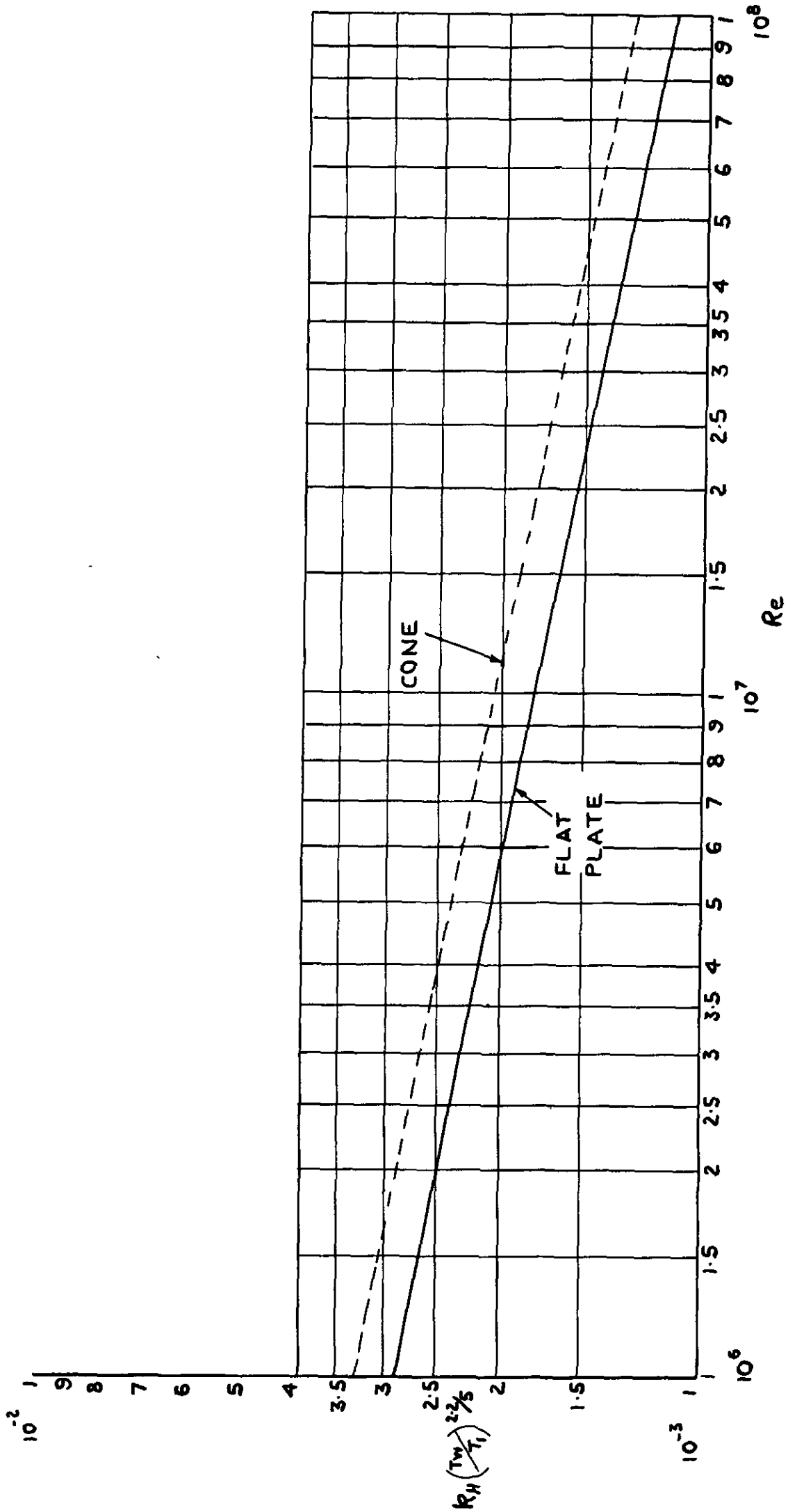


FIG 7.b. HEAT TRANSFER COEFFICIENTS FOR THE TURBULENT BOUNDARY LAYER.

FIG.8.a.

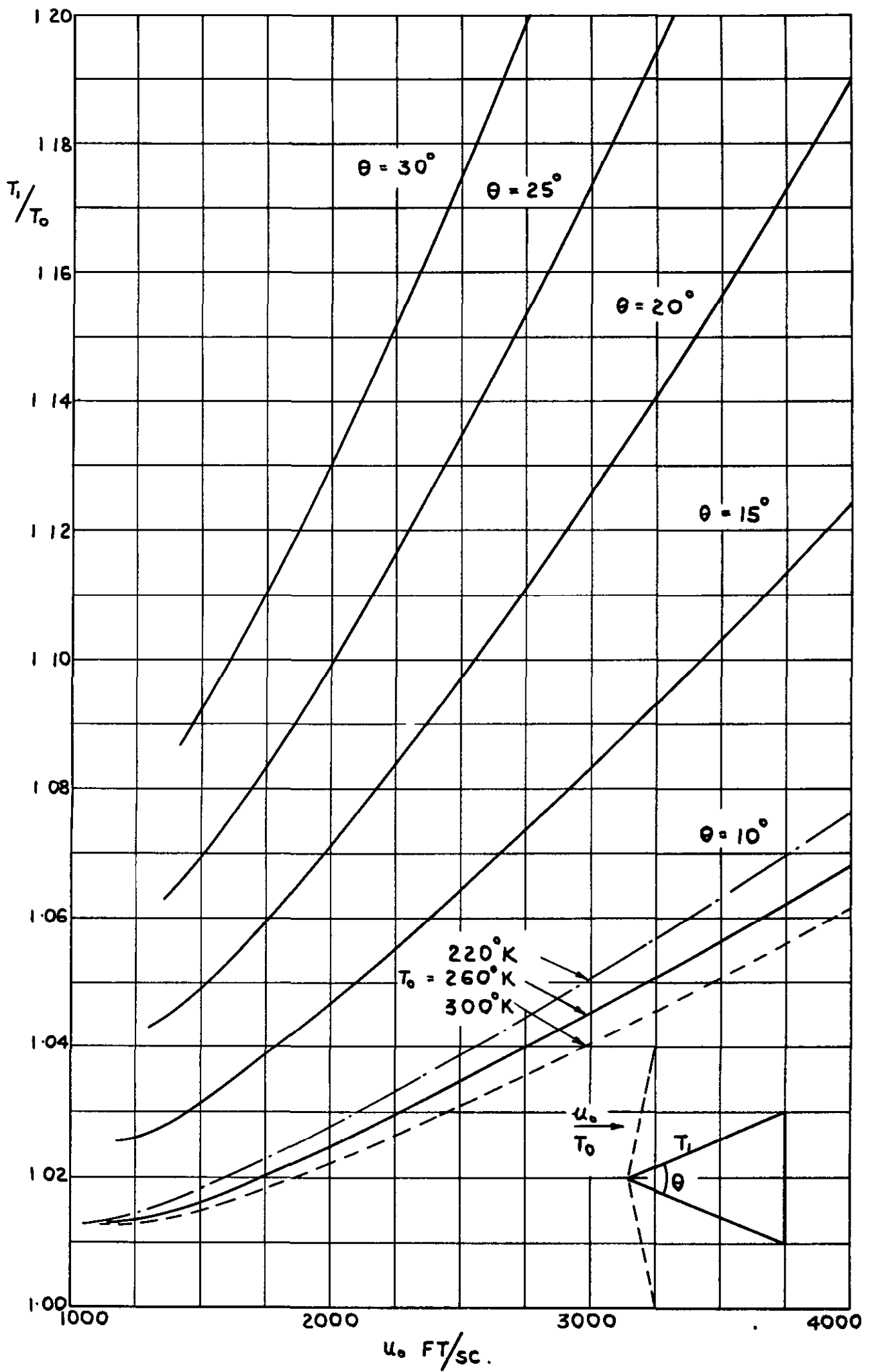


FIG.8.a. STATIC TEMPERATURE AT SURFACE OF CONE.
(STANDARD CURVES FOR $T_0 = 260^\circ\text{K}$.)

FIG. 8 b

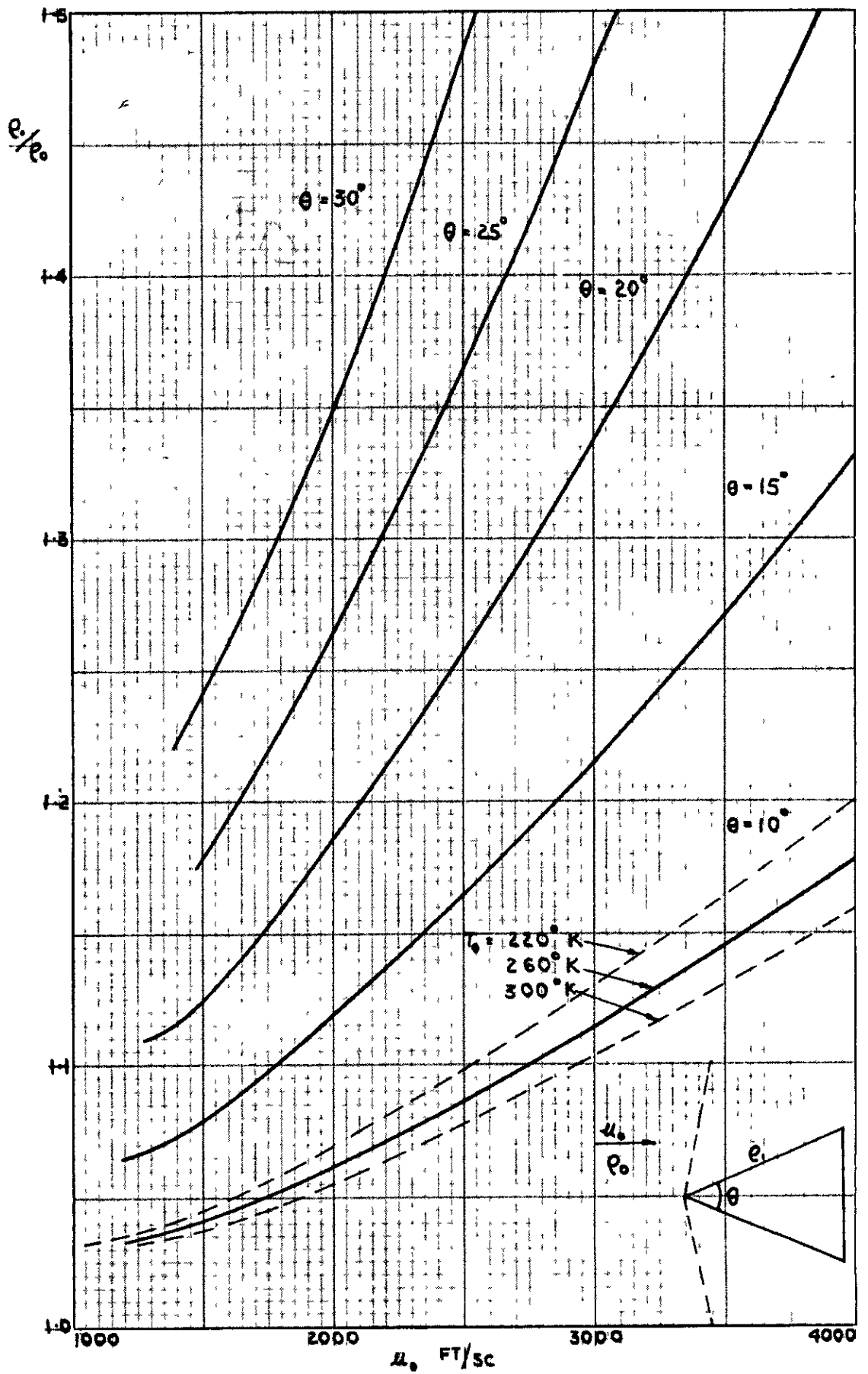


FIG. 8 b DENSITY AT SURFACE OF CONE.
 (STANDARD CURVES FOR $T_0 = 260^\circ\text{K}$)

FIG.8c

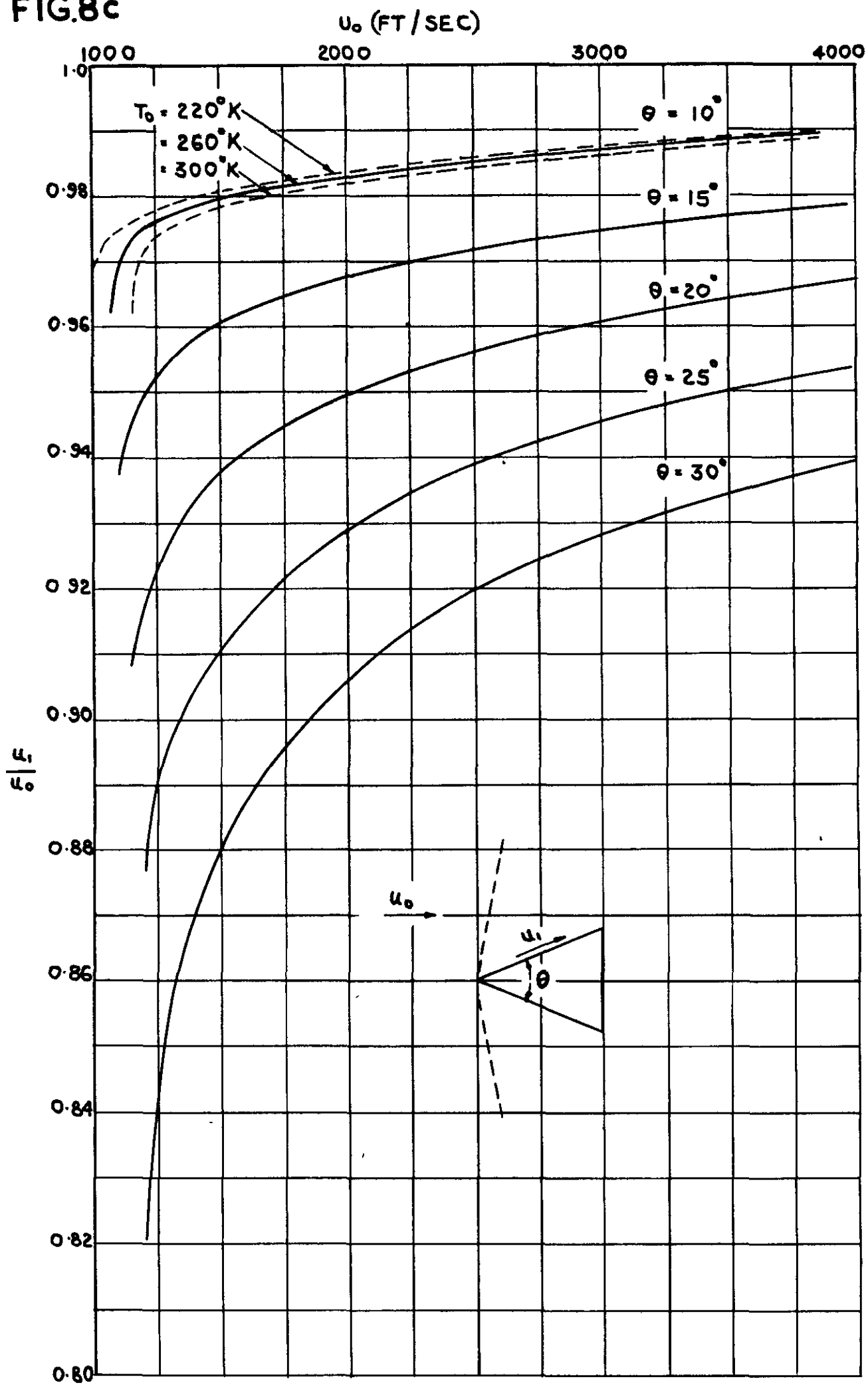
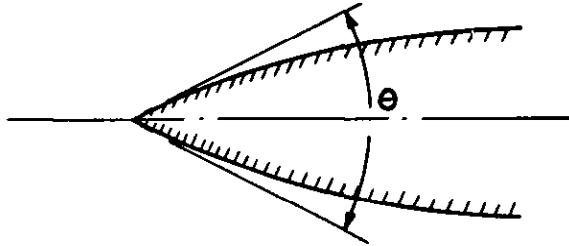


FIG 8c. VELOCITY OVER CONES.
(STANDARD CURVES FOR $T_0 = 260^\circ\text{K}$.)



$$(R_H)_{OGIVE} = (R_H)_{FLAT PLATE} \times \beta$$

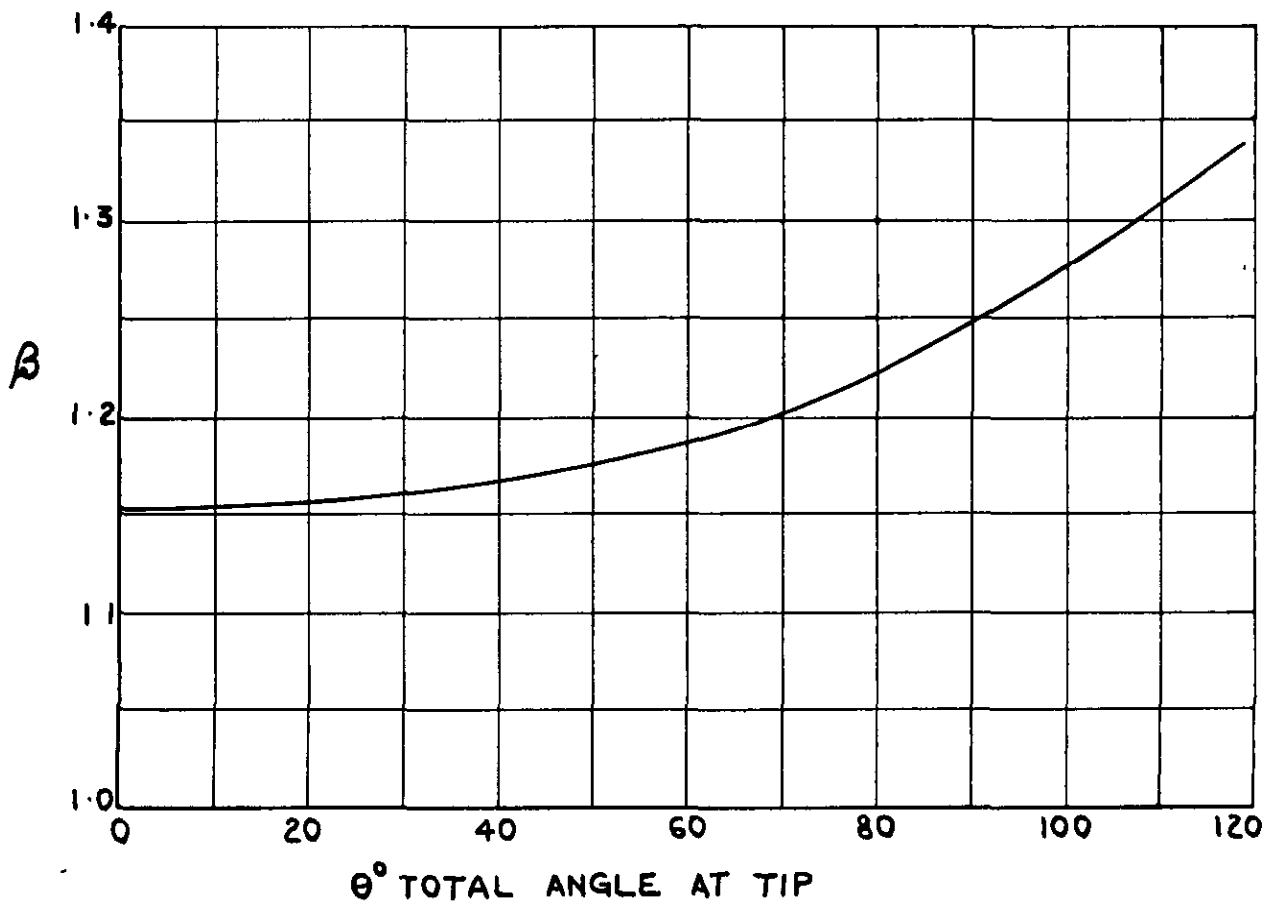


FIG.9. THEORETICAL RELATION BETWEEN THE BOUNDARY LAYER CHARACTERISTICS OF A TANGENT OGIVE & A FLAT PLATE.

FIG 10.

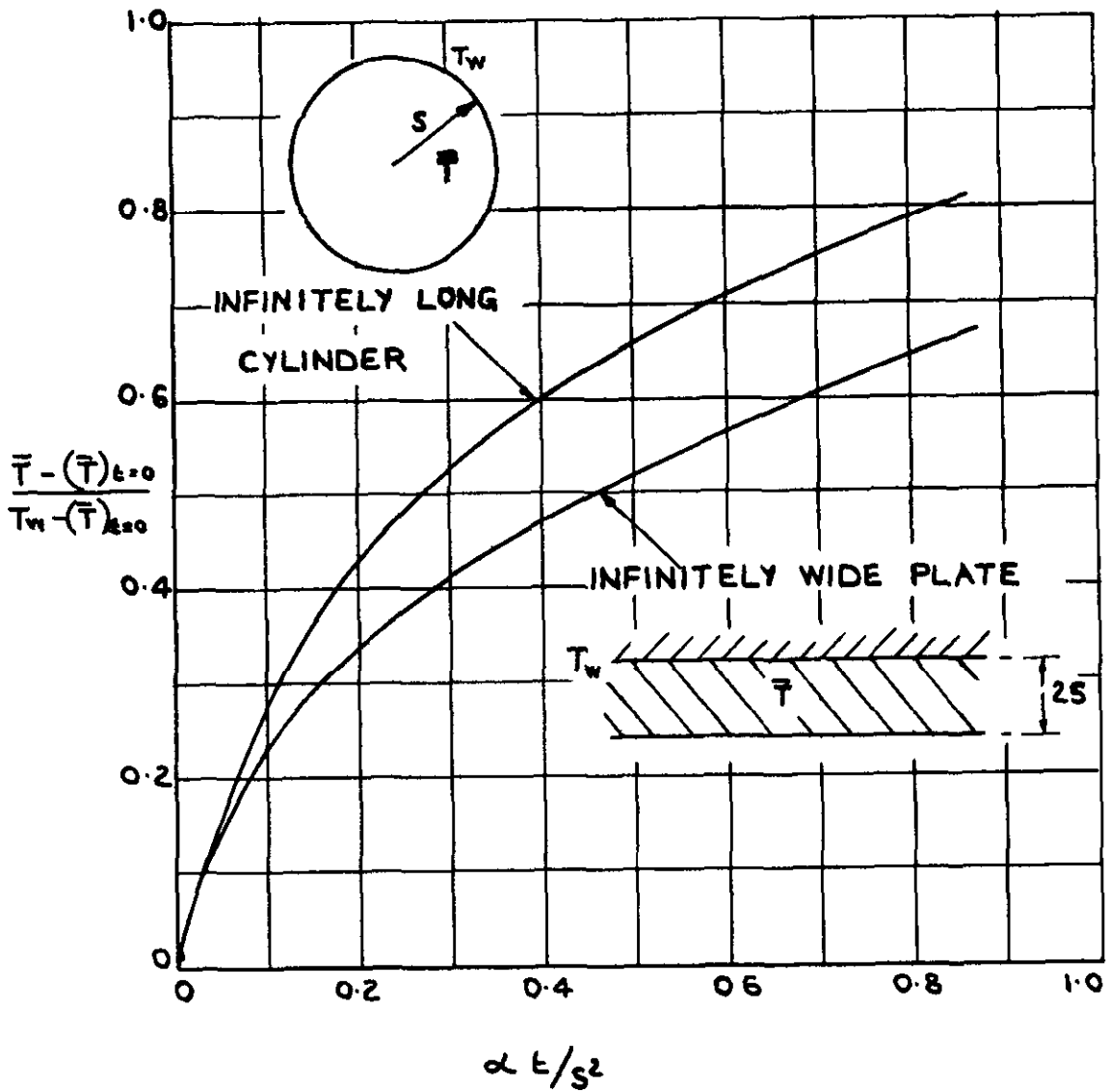


FIG.10. VARIATION OF AVERAGE TEMPERATURE \bar{T} OF AN INFINITELY LONG CYLINDER & AN INFINITELY WIDE PLATE ASSUMING A LINEAR VARIATION OF SURFACE TEMPERATURE T_w WITH TIME.

FIG. 11.

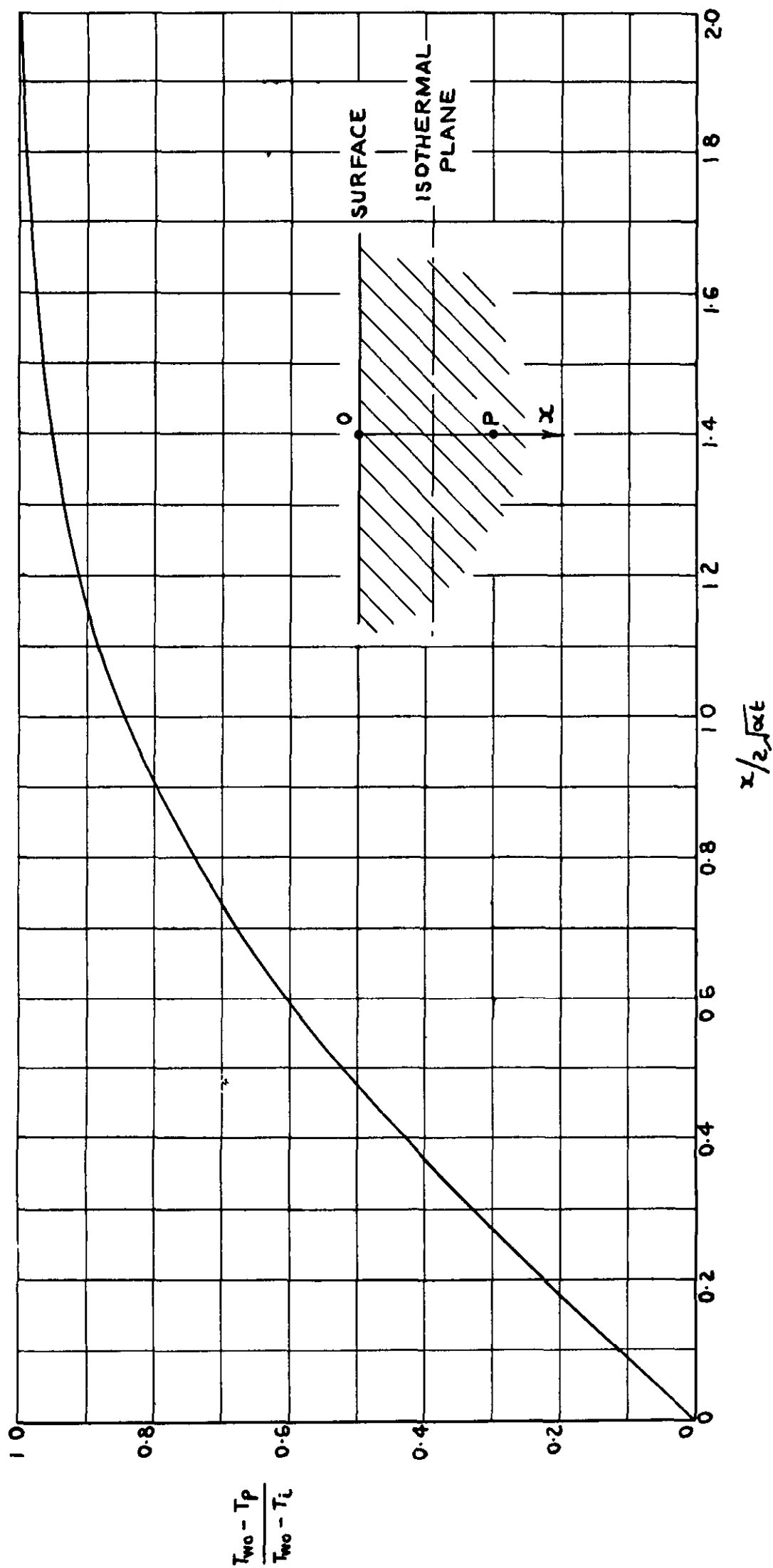


FIG. 11. TEMPERATURE SPACE TIME DISTRIBUTION THROUGH A SEMI INFINITE BODY.

FIG.12.

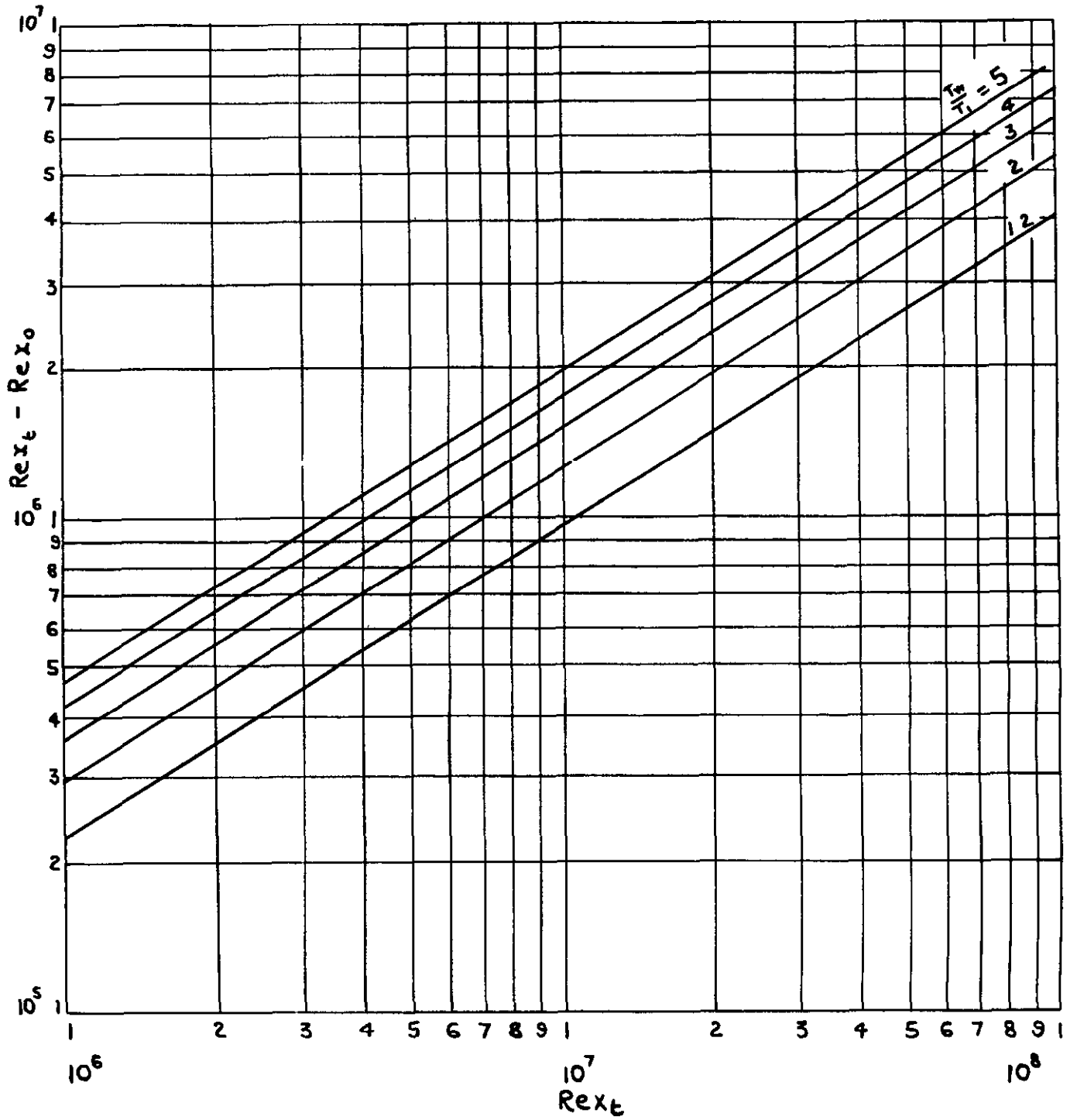
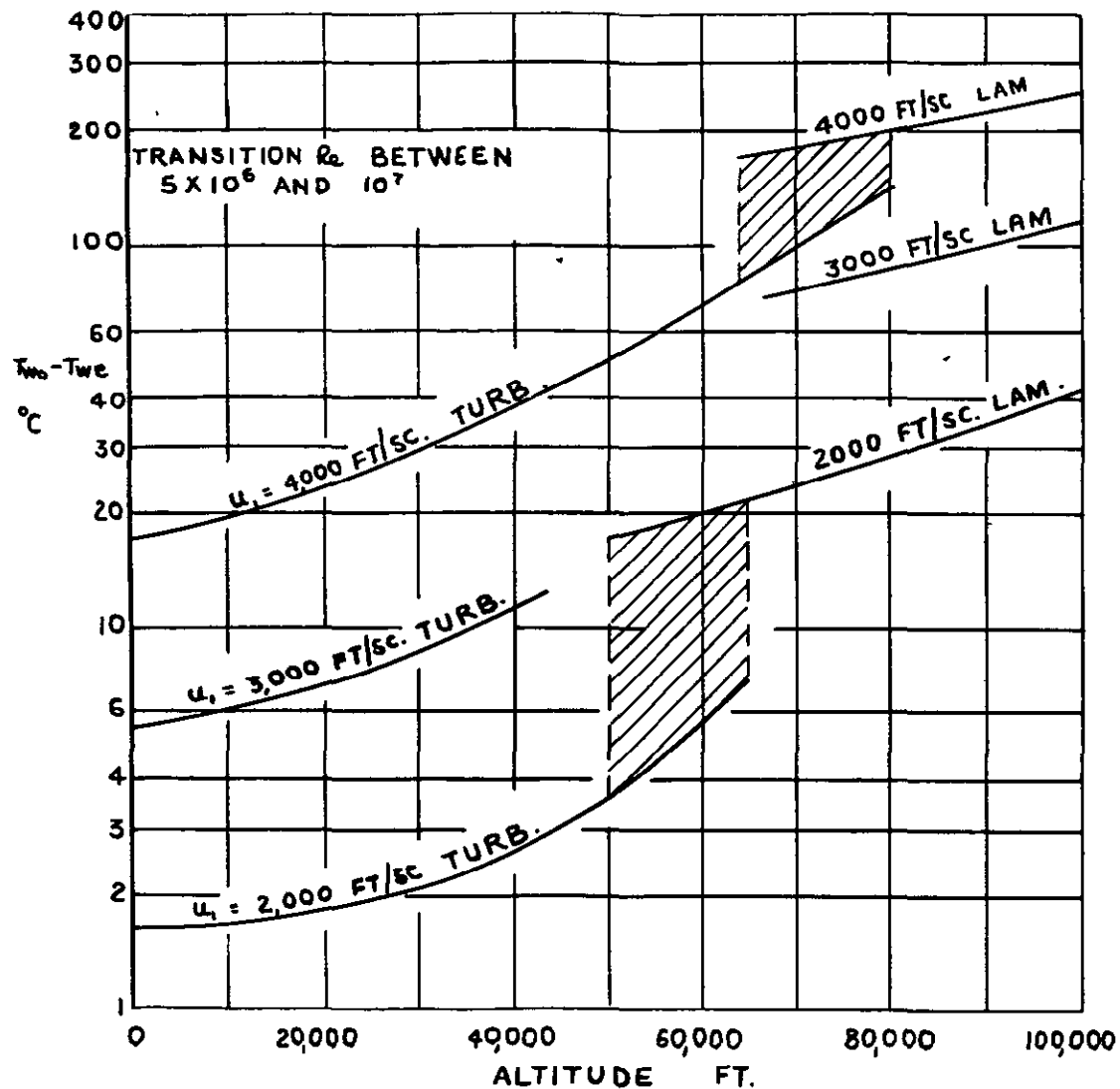
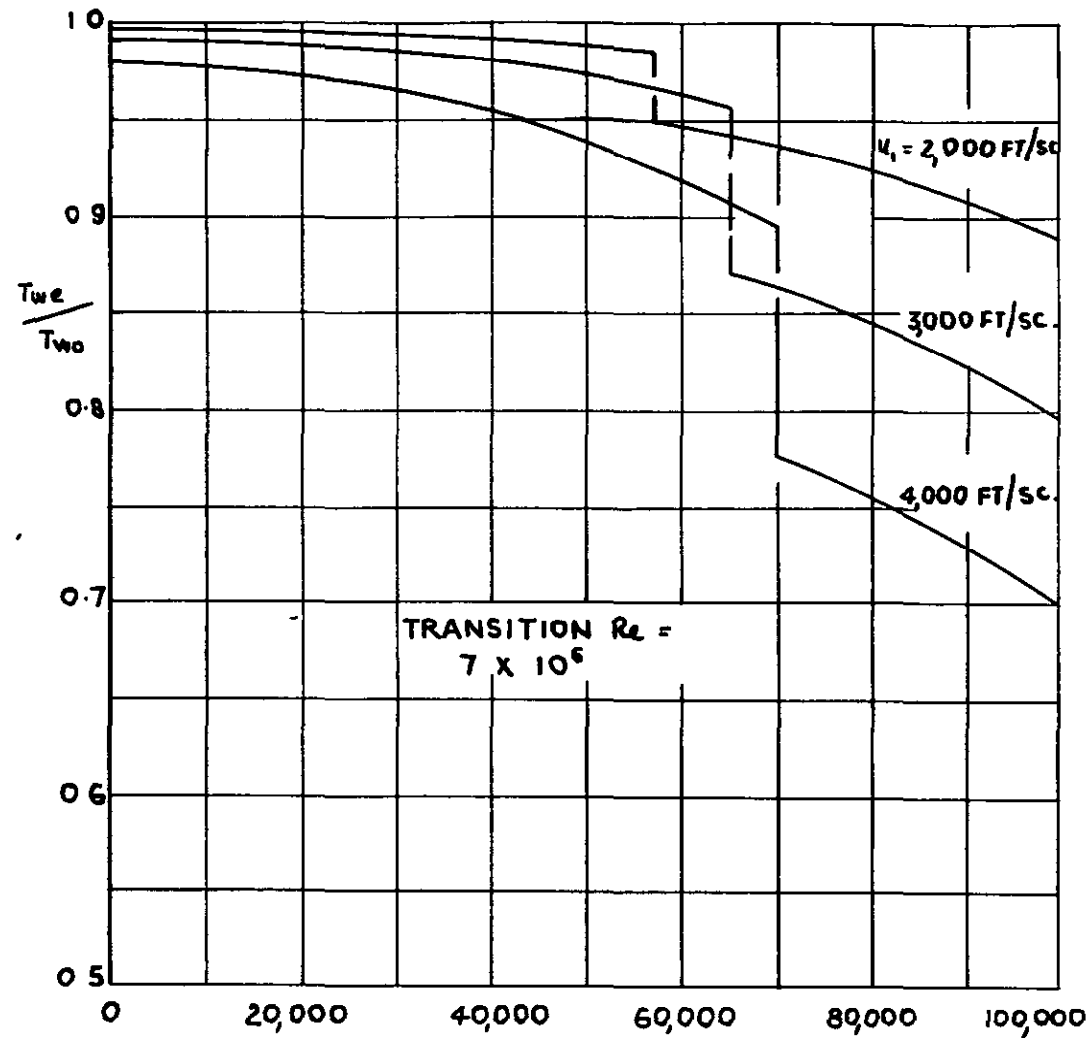


FIG.12. VARIATION OF $Rex_t - Rex_0$ WITH Rex_t



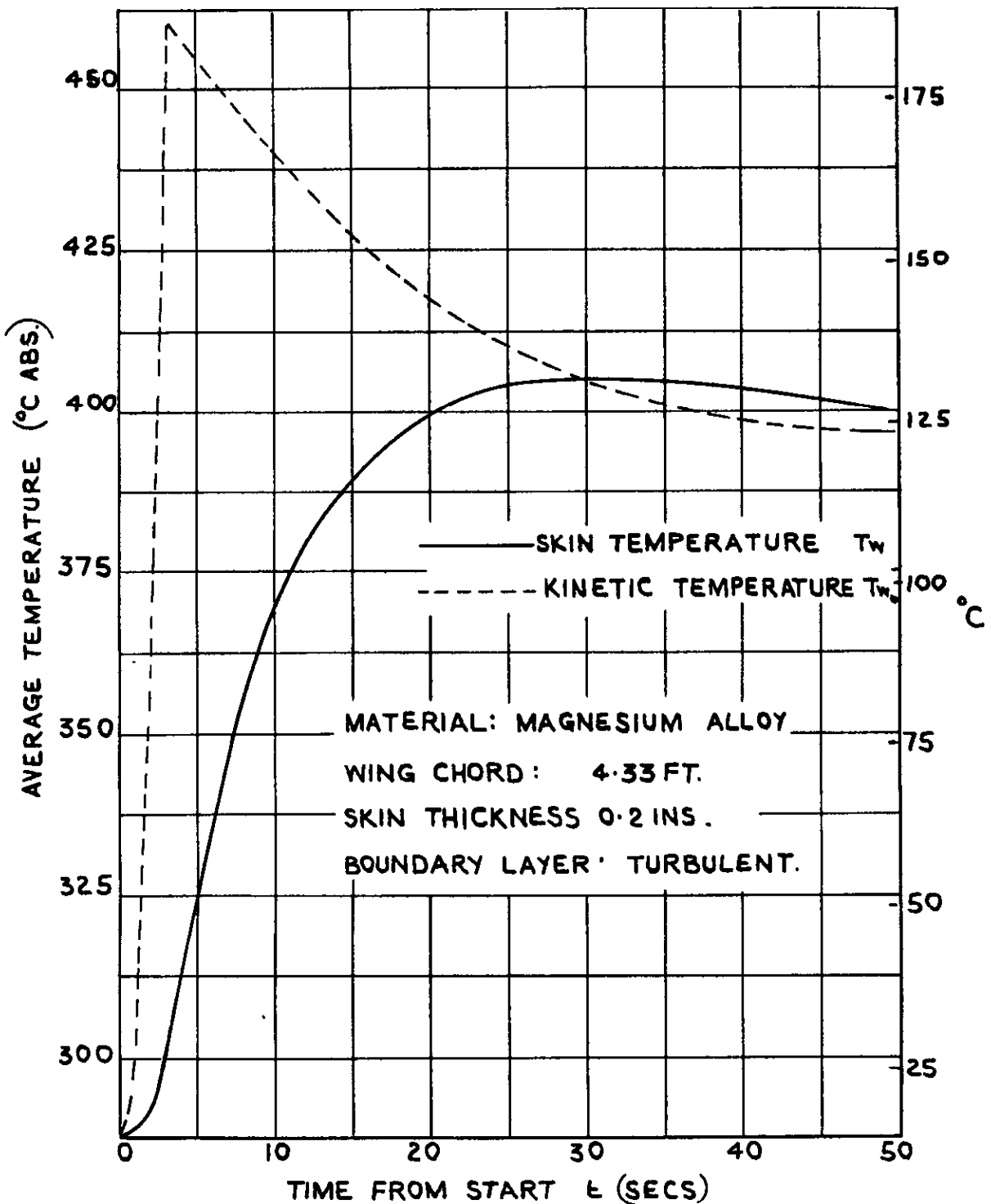
(a) TEMPERATURE DIFFERENCE



(b) TEMPERATURE RATIO

FIG.13 COMPARISON OF EQUILIBRIUM (T_{we}) AND KINETIC (T_{w0}) TEMPERATURES ON A 4 FT. CHORD WING OF EMISSIVITY, $\epsilon = 0.5$. (SOLAR RADIATION NEGLECTED.)

FIG.14.



VARIATION OF AVERAGE SKIN TEMPERATURE WITH TIME

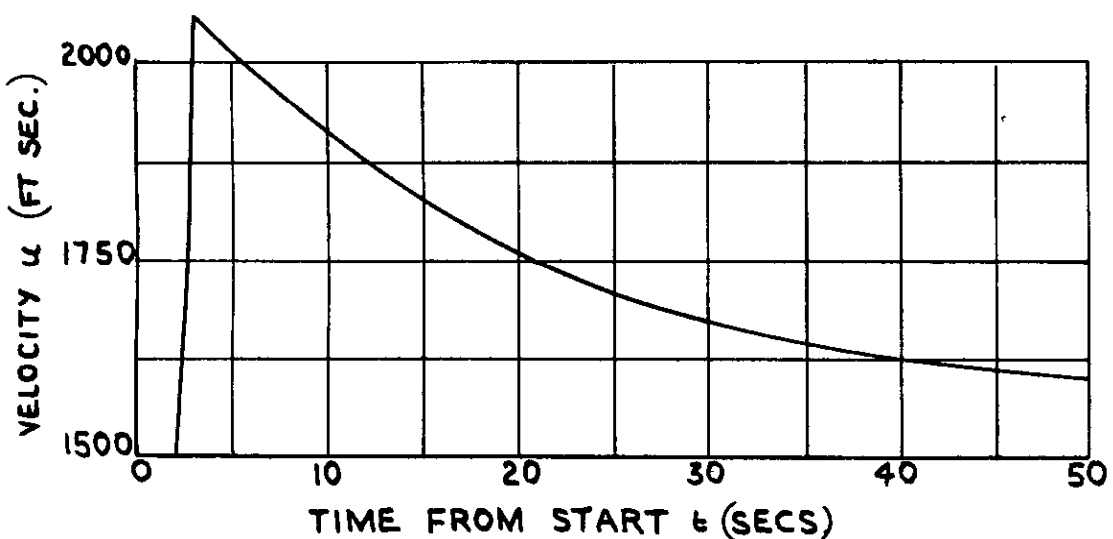
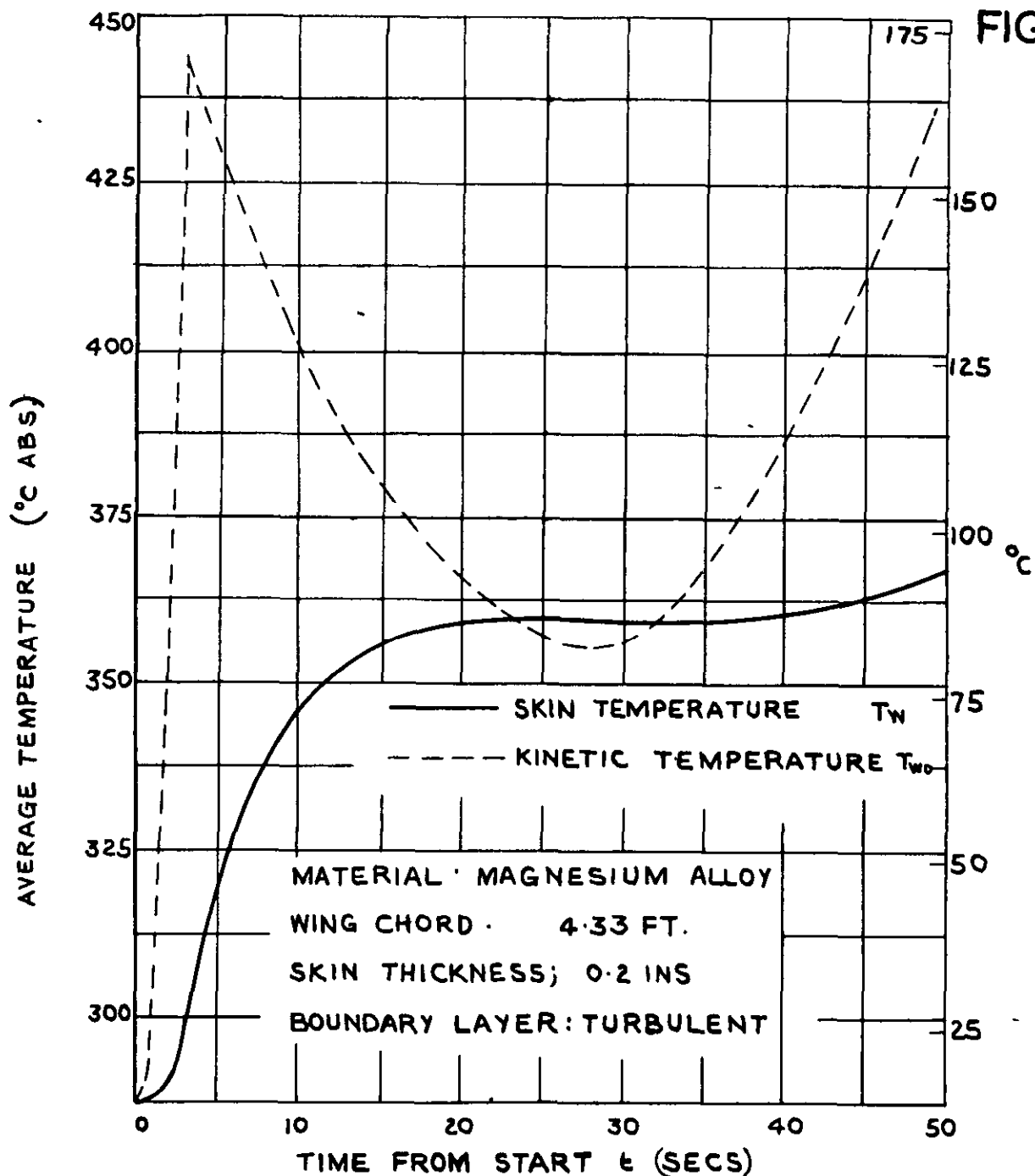


FIG 14. TRANSIENT SKIN TEMPERATURES FOR A FLAT PLATE WING IN ACCELERATED FLIGHT AT SEA LEVEL. (CASE A)

FIG. 15



VARIATION OF AVERAGE SKIN TEMPERATURE WITH TIME

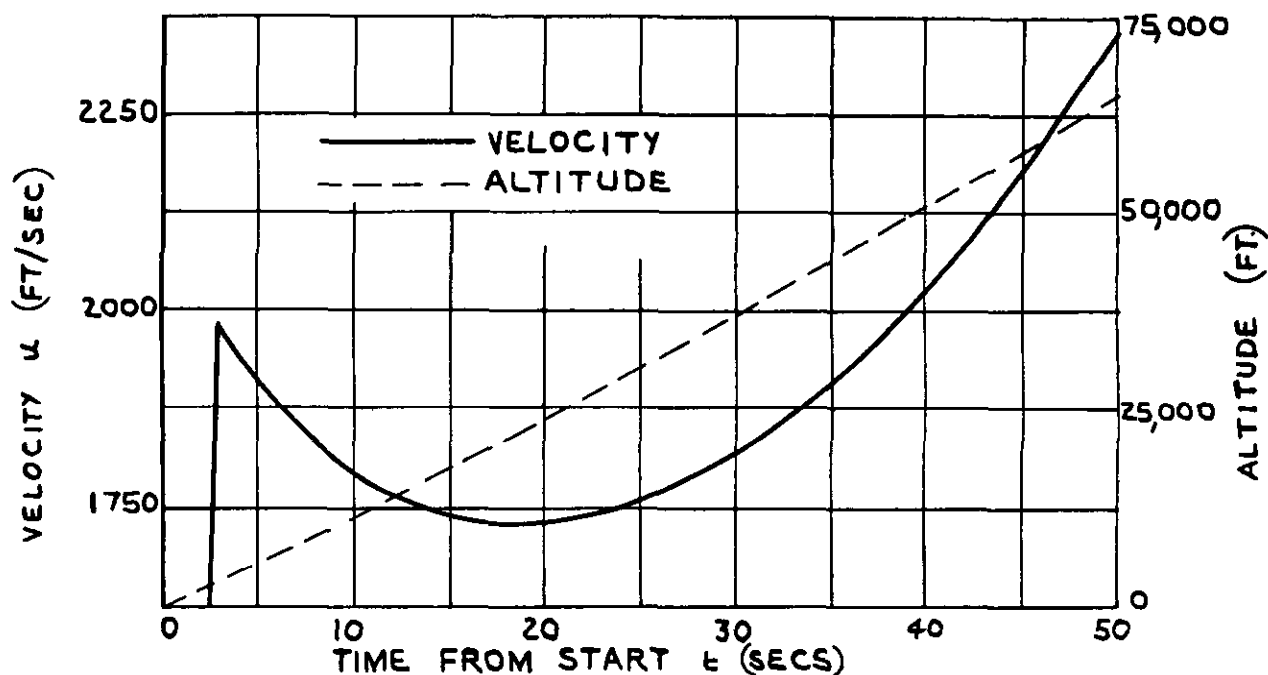
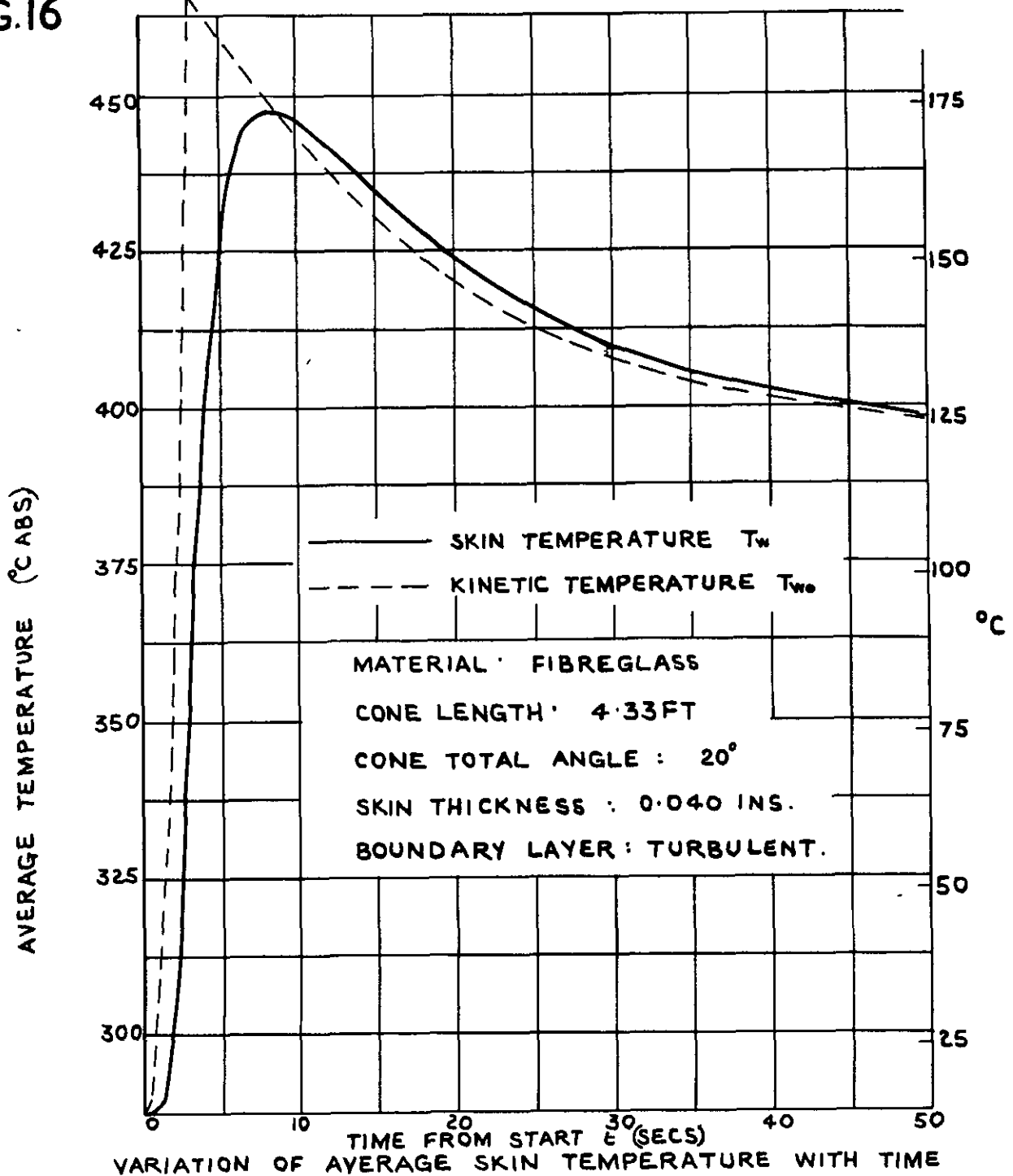


FIG. 15 TRANSIENT SKIN TEMPERATURES FOR A FLAT PLATE WING IN ACCELERATED FLIGHT AT VARYING ALTITUDE (CASE B)

FIG.16



VARIATION OF AVERAGE SKIN TEMPERATURE WITH TIME

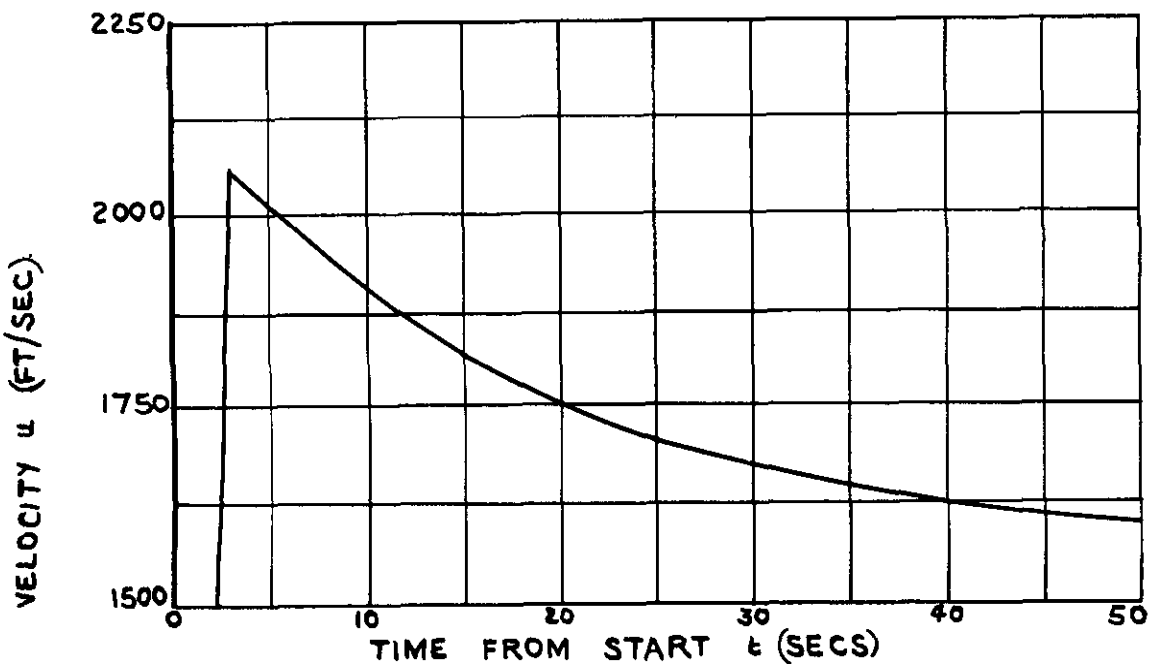
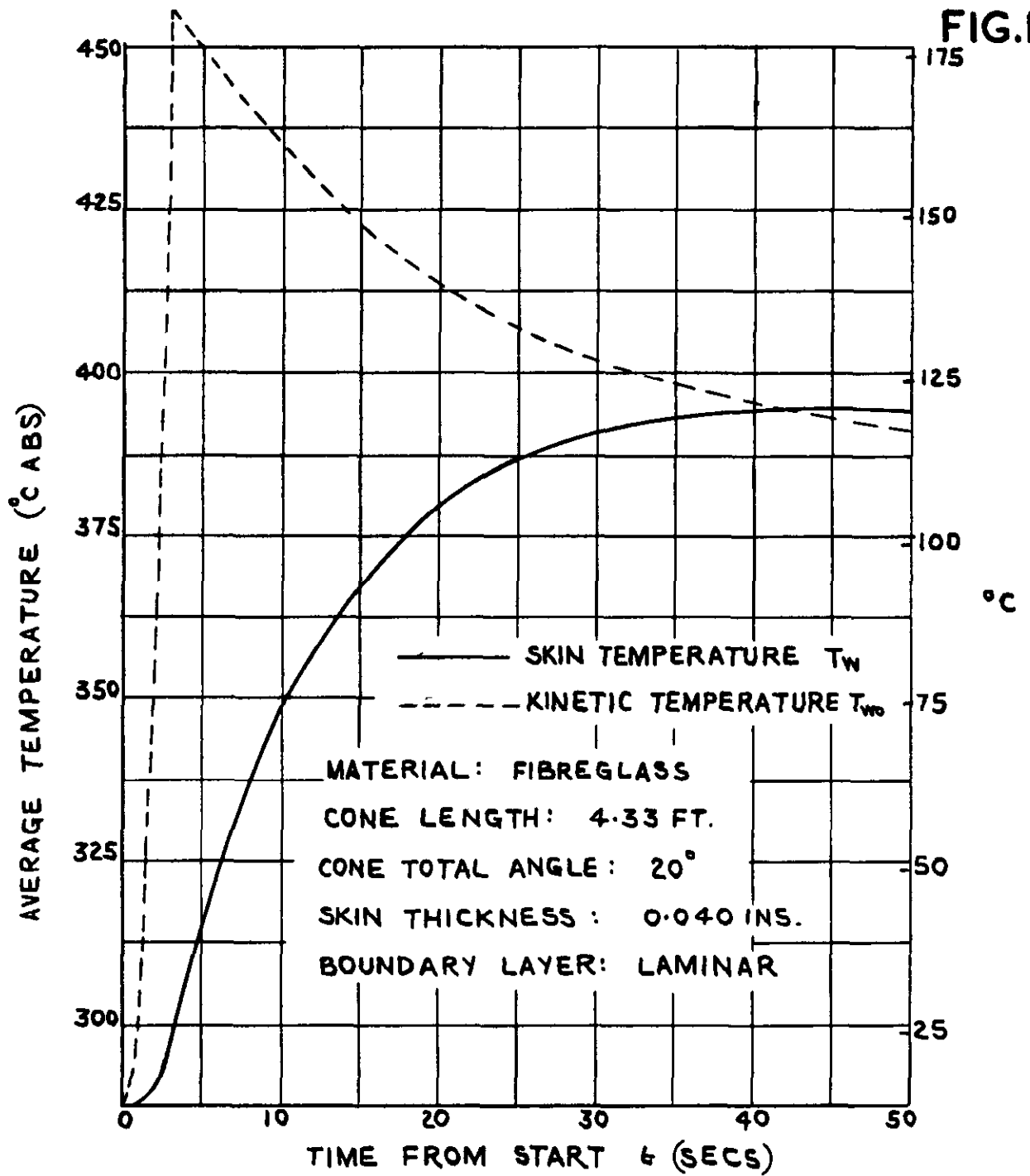


FIG.16 TRANSIENT SKIN TEMPERATURES FOR A CONICAL FOREBODY (TURBULENT BOUNDARY LAYER) IN ACCELERATED FLIGHT AT SEA LEVEL (CASE C)

FIG.17.



VARIATION OF AVERAGE SKIN TEMPERATURE WITH TIME

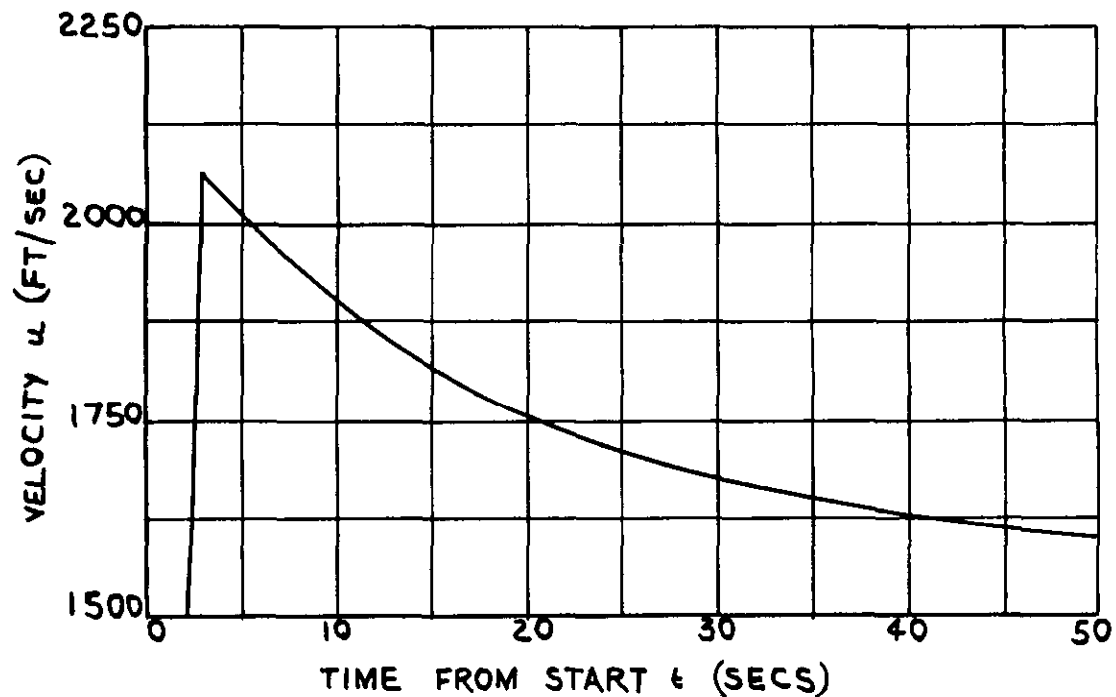


FIG.17. TRANSIENT SKIN TEMPERATURES FOR A CONICAL FOREBODY (LAMINAR BOUNDARY LAYER) IN ACCELERATED FLIGHT AT SEA LEVEL (CASE D)

FIG.18.

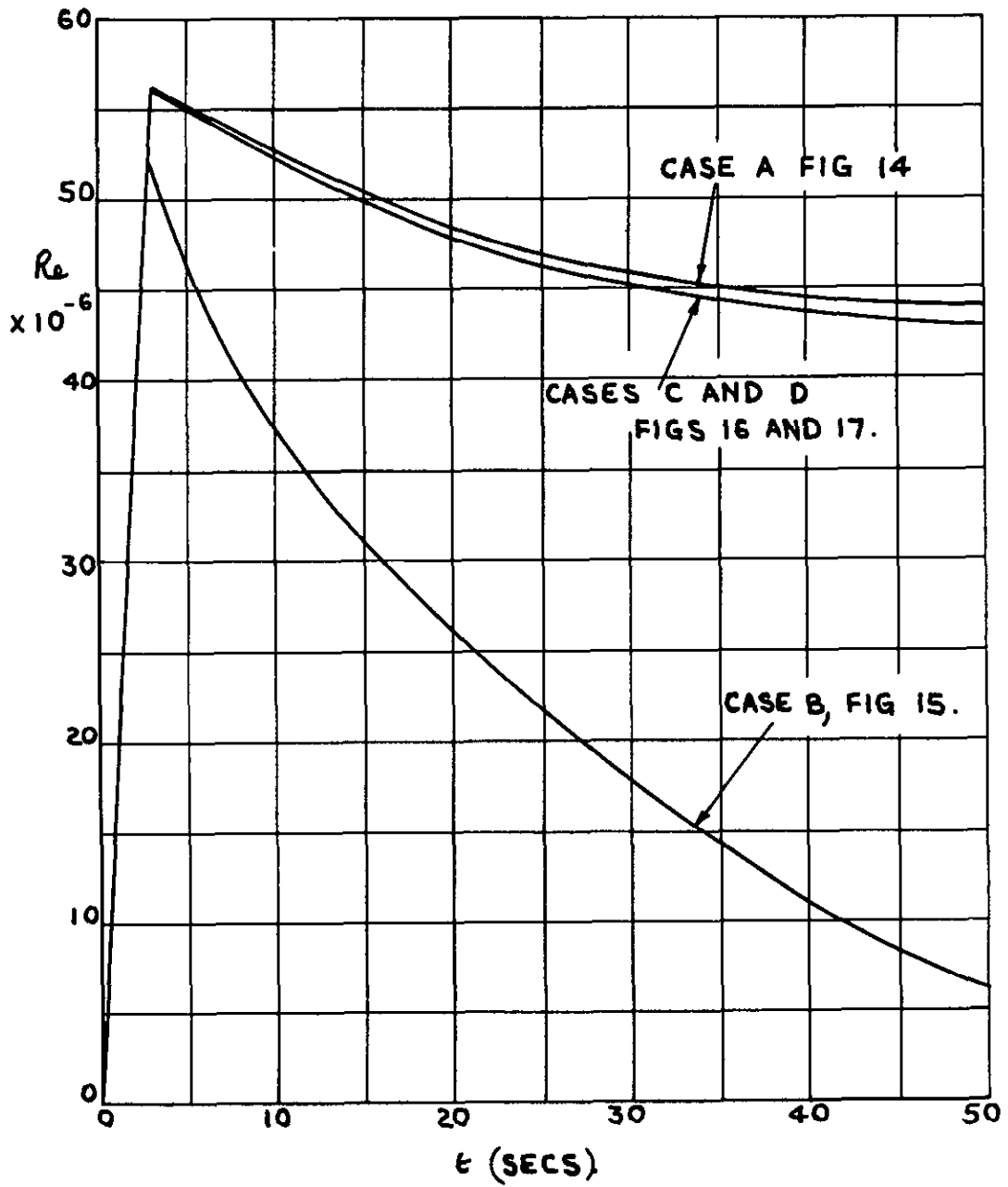


FIG.18. VARIATIONS OF OVERALL REYNOLDS NO ASSOCIATED WITH EXAMPLES IN FIGS 14-17.



Crown Copyright Reserved

PUBLISHED BY HER MAJESTY'S STATIONERY OFFICE

To be purchased from

York House, Kingsway, LONDON, W.C.2. 423 Oxford Street, LONDON, W.1

P O BOX 569, LONDON, S E 1

13a Castle Street, EDINBURGH, 2		1 St. Andrew's Crescent, CARDIFF
39 King Street, MANCHESTER, 2		Tower Lane, BRISTOL, 1
2 Edmund Street, BIRMINGHAM, 3		80 Chichester Street, BELFAST

or from any Bookseller

1953

Price 12s. 6d. net

PRINTED IN GREAT BRITAIN